ROBOTICS AND MECHATRONICS

DESIGN AND CHARACTERIZATION OF AN EMG BAND FOR DUCHENNE PATIENTS

P. (Philip) van de Maat

MSC ASSIGNMENT

Committee:
dr. ir. T.H.J. Vaneker
ir. M. Schouten
prof. dr. ir. G.J.M. Krijnen
dr. ir. K. Nizamis

December, 2022

050RaM2022
Robotics and Mechatronics
EEMathCS
University of Twente
P.O. Box 217
7500 AE Enschede
The Netherlands

UNIVERSITY OF TWENTE. | TECHMED CENTRE
UNIVERSITY OF TWENTE. | DIGITAL SOCIETY INSTITUTE

Summary

Duchenne muscular dystrophy (DMD) is a progressive muscle disease without a cure. Due to muscle degeneration, patients will slowly lose their arm functions. When the arm muscles are too weak to lift the arms, there are still electrical signals present in these muscles. These signals can be picked up using sEMG and used to drive an exoskeleton. In this report an sEMG band for the upper arm muscles is designed, 3d printed, and characterized. It can possibly be used to drive an exoskeleton in the future, to give DMD patients control over their arm functions again.

Some variables are tested to evaluate their effect on the sEMG signal. The infill percentage of the printed electrodes does not influence the signal (sEMG envelope, electrode impedance, signal-to-noise ratio, and standard deviation of impedance), as long as it is above 60 percent. The pressure with which the electrodes are pushed against the skin is not a deciding factor in creating a usable sEMG signal, as long as it is enough to keep the electrodes in their place. Although printable silver ink proves to yield a lower impedance and higher signal-to-noise ratio, it is more fragile than PI-ETPU. Therefore these materials are combined and printed on top of one another.

Four different prototypes of an sEMG band are developed and 3d printed. The final version features six electrodes, three on the triceps and three on the biceps. It can be adjusted with a watch band and is made almost entirely with a 3d printer. It can detect signals from both muscle groups. Testing by using the sEMG envelope of the band as the input for a computer game proves the band can be used accurately and quickly as a control system. This accuracy improves when integrating the envelope signal instead of only using the envelope as input.

Contents

1 Introduction

This report describes the work done by Philip van de Maat for his master thesis. In this introductory chapter the background of the work will be discussed, as well as related research, the stakeholders, and the typical user. It will provide the groundwork for the rest of the report.

1.1 Context

Duchenne Muscular Dystrophy (DMD), better known simply by the Duchenne illness, is a rare genetic disease that affects the muscles. In Europe and North America it affects approximately 6 per 100.000 males at birth, it is rarely seen in females [1]. Patients often show signs of weakened muscles before the age of 2. Muscle weakness will continue to increase and most patients are unable to stand up at the age of 12. The muscle weakness will continue and the average life expectancy with Duchenne is 26; although some people may live into their forties [2,3]. There is currently no cure, but physical therapy may help to ease the symptoms. Another development that is currently ongoing is the creation of braces with springs to lower the muscle strength required to, for example, lift an arm. Duchenne patients who normally would not be able to use their arm anymore, due to weakened muscles, may still be able to do so [4]. To use the current generation of exoskeletons the users still need to be able to move their arms. The next step could be to create an electrically driven exoskeleton, instead of the passive exoskeleton that exists now. This exoskeleton would still need a signal to derive the user's intended movement; surface electromyography (sEMG) is a method to detect these signals. In this paper an sEMG band is designed to detect signals from the biceps and triceps, so it can potentially be used to drive an exoskeleton in the future.

1.2 Related work

The idea to design an sEMG band to pick up signals from the muscles, and to later possibly drive an exoskeleton is not new and was already demonstrated in 1980 [5]. The use of 3d printing to produce sEMG electrodes has also been proven to yield good results [6]. Martijn Schouten, a Ph.D. student in the Wearable Robotics consortium working at the University of Twente, has developed a band for sEMG signals from the biceps. A picture of the band can be found in fig. 1.1. It uses flexible, 3d printed sEMG electrodes. This means the whole band can be 3d-printed with a Fused Filament Fabrication (FFF) printer [7, 8]. However, the band has some shortcomings. Firstly, the quality of the signal from the band is not sufficient. It can show large jumps in signal or it is very weak. Secondly, the band is not adjustable for different arms. Finally, the band is not aesthetically pleasing or inviting to use. These problems will be addressed in a redesign and improvement of the band.

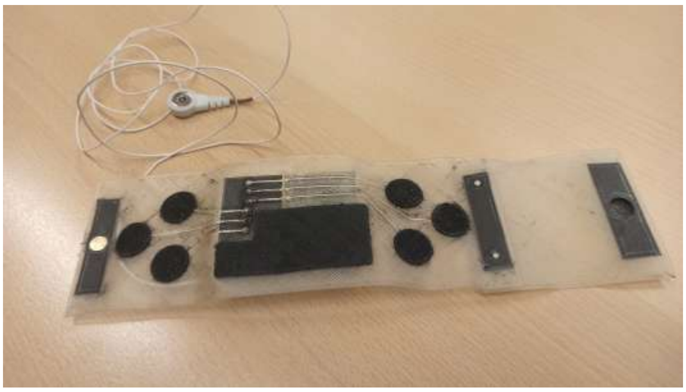

Figure 1.1: The sEMG band developed by Martijn Schouten.

It should first be explored whether or not sEMG is a viable control interface for patients with DMD. In a study by J. Lobo-Prat et al. [9], sEMG and force-based control interfaces are compared, and DMD patients are asked to perform test using both methods. The three test subjects did all succeed with their task using both methods. Although force-based controlled movements were smoother, sEMG was found to be less tiring for the subjects [9]. A follow-up study [10] concluded that force-based control interfaces are better for patients who still have enough strength in their arm, but sEMG is preferred by weaker patients since it is less fatiguing [10]. This study also conducted the tests with two degrees of freedom, compared to one in the previous study.

Instead of sEMG, other techniques can also be used to measure the signal from someone's muscles. Mechanomyography (MMG) is a technique that works by measuring vibrations in the muscles [11]. The signal-to-noise ratio of MMG is typically higher than of sEMG [12]. However MMG is only tested on healthy people with fully functioning muscles, while sEMG has been confirmed to work on DMD patients [10] [13]. Therefore sEMG is the better choice for an exoskeleton driver at this stage.

Another interesting technique is high-density sEMG (HDsEMG). An sEMG measurement is called high density, rather arbitrary, when more than 16 electrodes are used [14]. Because of the high number of electrodes, the exact placement of a single electrode is less critical, since there will always be some electrodes with the strongest signal [15]. This could be interesting for DMD patients, since they can potentially wear their sEMG bands for a long time, thus increasing the chances for the electrodes to shift.

HDsEMG has been tested on Duchenne patients, where it was found that DMD patients activated fewer electrodes than healthy subjects, and had contractions closer to their maximum contraction [16]. However, using a 3d printer to print an HDsEMG band would require a controller that can use at least 17 inputs (16 plus a ground). For this project it is chosen to use an existing controller that has 7 inputs (more information on this controller can be found in section 2.4), thus HDsEMG is not an option at this point.

Some doubt has been cast on whether DMD patients still produce strong enough sEMG signals to pick up and process. A study by J.Lobo-Prat et al. found that a patient with DMD who lost his arm functions 15 years ago, still had measurable sEMG signals [17]. The amplitude of the signal was a factor 100 lower than of a healthy subject. It was concluded, however, that this was potentially enough to use in a control system.

1.3 Approach and report structure

In an article by A. Kappeller et al, a socio-philosophical perspective on wearable robotic exoskeletons (WRE's) for patients with DMD is given [18]. The article concludes with two recommendations for the development of WREs, which can be useful for the development of the sEMG band, namely: "the involvement of patient organizations and a participatory approach to design can help reduce ableist ideas, and the provision of modular design and choices can help reduce the stigma attached to WREs" [18]. These recommendations should be kept in mind, especially during later stages of development.

The report is divided into various chapters. In the introduction, the problem and its context are explained. In the problem analysis chapter, the stakeholders and typical user are shown, and from these, the requirements are formulated. In the design chapter the different prototypes are showcased and, more importantly, how these designs came to be. In the fabrication chapter the technical details regarding how the band was produced are discussed, so it should be possible to recreate it. In the measurements chapter it is explained how the band is tested and what data is recorded. These results are then listed and discussed in the results and discussion chapter. Finally, in the conclusion chapter, the key findings from the report are discussed and recommendations for further research are done.

2 Problem Analysis

In this chapter, the problem will be further looked into. This is done by conducting a stakeholder analysis, creating a typical user profile, and formulating the requirements.

2.1 Stakeholders analysis

Stakeholder groups

The identified stakeholders can be seen below, in no particular order:

- Duchenne patients
- Family/carers of patients
- Wearable Robotics
- TMSi
- Healthcare insurance
- Yumen

In figure 2.1 a power interest graph is displayed. It shows the power over, and the interest in, the project of each stakeholder. It is important to keep in mind that this graph is based on a fully finished, marketable product. It may still take years to reach this stage, or the project could never reach it. Their location in the graph determines how the stakeholders will be treated. This relationship is listed in the legend on the right side of the diagram. In the next section, the stakeholders will be discussed further.

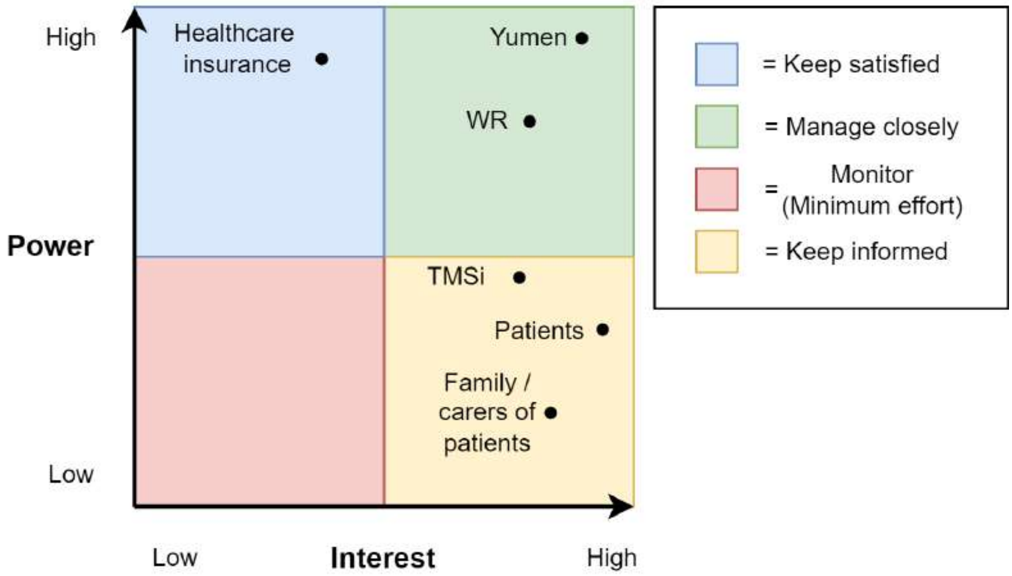

Figure 2.1: Connections between the different stakeholders.

2.1.1 Stakeholder intentions and power

In this section, the intentions, motivations, and power that each stakeholder has over the project will be discussed. It is important to know this since stakeholders can greatly influence a project.

Duchenne patients

Of course, the Duchenne patients should be the most important people in the research since the product is developed for them. They want a technical solution so their quality of life gets improved. The main way they can influence the final product is by giving feedback in the testing phase. They have the power to drastically change a design if, according to their opinion, it does not work (well). This means they have moderate power over the project, but great interest in the project.
However, it is chosen not to include the patients in the design of the band yet. This is done so patients don't have unrealistic expectations of the project since it would most likely take years before a complete product has been developed.

Family and carers of Duchenne patients

The family and carers want the best for the patients, so their motivations largely overlap with the patients themselves. However, since they are tasked with caring for the patients, they want that care to be easy and quick (assuming the quality of life for the patients is not in danger). Therefore a technological solution that makes a Duchenne patient more independent gives the carers more free time. At the same time these people will have to put the final product on the patient, and maybe do some basic maintenance. They should not be forgotten in the testing phase. They have little power over the project, however, they can influence testing.

Wearable Robotics

The Wearable Robotics project is carried out by a consortium including the University of Twente, the Technical University of Delft, the Radboud University Nijmegen, the Free University Amsterdam and a collection of companies ranging from tooling to medical companies. They research and develop technology to improve or bring back human motor functions. Their development may not always align with the patients, who simply want a quick product on the market. The Wearable Robotics consortium may take steps in development that are not necessarily needed for the development, thus slowing down the final product. Another possibility is that a final product will never be developed, and the development stops before it is completed. This gives the Wearable Robotics consortium the most power over the product and process.

TMSi

Martijn Schouten (Wearable Robotics) designed the electronics (Octopus) of the band, and TMSi reviewed it. They also partly funded the research, and because they could decide to cut the funding, they have some power over the project. However, the electronics could also be produced somewhere else.

Healthcare insurance

Healthcare insurance providers can make or break a product. If the product will be too expensive, they might simply not cover it. So their power is large. Therefore it is important to start communication with them early, to make sure the product will reach the patients in the end, and be covered by the healthcare providers.

Yumen

Yumen Bionics is founded by the Duchenne Parent Project Netherlands to fund research and produce technical solutions for Duchenne patients. Yumen wants the best for the Duchenne patients, so their motivations largely overlap with the patients themselves and their families/-carers. But they also need green light for their product from the healthcare insurance. Their power is large since they are the party that might market the product in the end. Their interest is also large since their motivations overlap with the patients.

2.2 Context of usage and typical user

Before making a list of the requirements it is important to know in what setting the band most likely will be used. Almost all DMD patients are male, [3] therefore the band will be tested on males. Because Duchenne is a progressive illness most patients will be in a wheelchair by the time they are 12 years old [2]. Children with DMD can often live with their parents but as the illness develops and the care required increases most patients will live in an assisted living environment. They require extensive care and attention with activities of daily living. They also have sensitive skin and require physical therapy to keep their joints working as much as possible. Patients have a thinner upper arm compared to healthy individuals, especially when they are higher on the Brooke scale [3].
In short, the typical patient the band will be designed for is the following:

- Male
- Adult
- Unable to walk, in a wheelchair
- Living in an assisted living facility
- Has a score of 5 or 6 on the Brooke scale, meaning they can at most hold a pen or pick up pennies from a table, but cannot move their hand to their mouth
- Has sensitive skin
- Gets daily physical therapy
- Has a smaller diameter upper arm than a healthy individual

A 5 to 6 score on the Brooke scale indicates extreme conditions. Someone with a score of 5 on the Brooke scale cannot use a passive brace with springs, while someone with a score of 4 can. Therefore the band is designed for patients with a score of 5 or 6.

2.3 Requirements

When making a list of the requirements, it is important to start with the technical ones. The band should provide a good, constant reading of sEMG signals, so that it can reliably drive an exoskeleton. In table 2.1 all requirements, the way to test them, and their thresholds are listed. They are divided into three different categories: technical, safety and usage requirements. To make it easier to refer to they are numbered. Below, the requirements will be further elaborated on. It should be noted these requirements are for a finished product and do not apply to prototypes.

2.3.1 Technical requirements

First, some technical requirements are needed to ensure a good quality signal. Here the signal-to-noise ratio will be calculated in dB. The noise is the signal when the muscles are relaxed, while the signal is the signal when the muscles are contracting. A stable signal is also important, this is measured by looking at the impedance standard deviation. When the standard deviation is low, the signal is more stable. The band should also have a rechargeable battery, which is better for the environment, cheaper in the long run, and easier for the user compared to using non-rechargeable batteries.

The band should function for an extended time on one battery, to make sure the user does not have to recharge the battery often.

2.3.2 Safety requirements

From section 2.2 it follows that the typical user has sensitive skin. Therefore there should be no sharp edges on the band so the chance that the skin will be damaged is minimal. It is also important to use materials that are safe to use in contact with human skin.

Another requirement is to make sure that the device is splash water resistant. When worn for an extended time, water could accidentally be dropped on it, and the band should still be working afterward.

2.3.3 Usage requirements

Finally, there are some requirements that make the band easier to use. It should be easy and quick to put the band on or take it off. Because the typical user lives in an assisted living facility, the caregivers should not be overburdened. The band should be adjustable. From the typical user it follows that DMD patients often have a smaller diameter arm compared to healthy individuals, but this varies per patient.

The band should also be inviting to use, so it is easier for the patients to decide to use it. Of course, the comfort for the patient is also very important, thus the band needs to be comfortable, also for extended wearing times.

The band should also be easy to clean. Ideally, this should be done in a dishwasher, so it is as easy as possible for the caretakers. Lastly, the band should be impact-proof. It is very likely that at some point the band will be dropped, and it should be able to withstand that.

Table 2.1: Table with requirements for the sEMG band.

Number	Requirement	How to measure	Threshold
	Technical requirements		
T1	Transmit good quality sEMG signal	Measure the ratio of the signal to the noise	At least a ratio of 10 (20 dB)
T2	Transmit a constant sEMG signal	Measure the impedance standard deviation	At most 5% of the impedance
T3	Be rechargable	Check if the battery can be recharged	It should be able to
T4	Can function for an extended time	Measure the time before the band stops working	A minimum of 4 hours
	Safety requirements		
S1	No sharp edges on the band	Feel if there are sharp edges on the band	Maximum of 0 sharp edges
S2	Use materials safe for contact with human skin	Request material information from the manufacturer	Only use medically certified materials
S3	Be splash water resistant (IPX4)	Pour small quantities of water on it (3x 2 mL)	The band and electronics should function after
	Usage requirements		
U1	Be easy to put on or take off by a different person	Measure the time how long it takes to put on, or take off the band	Less than 1 minute
U2	Be adjustable for different arm sizes	Put the band on different people and see if it fits	Fits at least 80 % of the subjects
U3	Be aesthetically pleasing and inviting to use	Ask different people how they would rate how good the band looks on a scale from 1 to 10	At least a 7/10
U4	Be comfortable to wear for the patient	After wearing the band for 10 minutes, test subjects should describe how comfortable the band is on a scale from 1 to 10	At least a 7/10
U5	Should be easy to clean in a dishwasher	After removing the electronics: Put the band in a dishwasher	The band should still work after the dishwasher
U6	The band should be reusable	See if the band can be used for multiple sessions	At least two 30 minute sessions
U7	The band should be impact proof	Drop the band from a height of 2 meter 10 times	No significant damage afterwards

2.4 Electronics

The band will be designed around an existing amplifier, called the Octopus, shown in fig. 2.2. It consists of the Texas Instruments ADS1298 Analog Front-End chip, connected to an NRF52832 Bluetooth low energy (BLE) module, which can send data wirelessly, in real-time, to a computer. On the computer, a custom Python program can read, display, and save the data. The device has a battery inside and can charge wirelessly. There are seven pogo pins on the underside. This makes the Octopus ideal for usage in a 3d printed band since once it is in a suitable box, the pins will press down on the print. This means it is easy to connect the Octopus to the 3d printed part of the band.

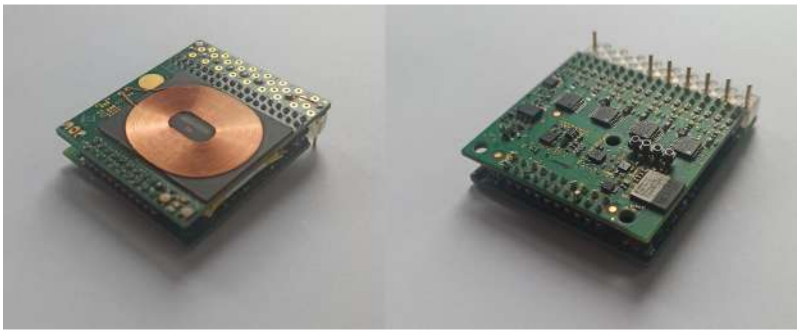

Figure 2.2: The top (left) and bottom side (right) of the Octopus amplifier.

2.5 Conclusion

In this chapter, the requirements have been formulated. They are used to design the prototypes of the band, this can be found in the next chapter.

3 Design

In this chapter, the design of the bands will be elaborated. It will be detailed how the designs follow the requirements, and what the differences between the versions are.

3.1 sEMG bands

3.1.1 sEMG band: version 1

As for the first design, before printing, not much can be said about requirements T1 and T2, since these properties can only be evaluated after printing.

The safety requirements can be evaluated beforehand, by carefully choosing the materials and making the design. It is chosen to not make the design splash water resistant at this stage (requirement S3) since it takes much time, and the band will also change significantly. It is also very hard to evaluate this since the chance of destroying the Octopus is high. The same applies to requirement U7, making the band impact-proof.

The usage requirements are very important for the design. A watch band is chosen to secure the first prototype, because it can create a secure connection, is easy to connect and disconnect, and is adjustable so it can fit different arm sizes (requirements U1 and U2). This will also make sure the band will be more comfortable since the user can adjust how tight the band is around their arm (requirement U4). A design with rounded edges is chosen since it is expected that people will find this more aesthetically pleasing (requirement U3). By making it easy to remove the Octopus, it is possible to clean the band in a dishwasher (requirement U6).

The first prototype version of the band can be seen in fig. 3.2. It features three electrodes, with silverink CI-1036 (Engineered Materials Solutions, Inc.) on top of PI-ETPU 85-700+ as connections to the octopus. The silverink is a viscous ink, with a very low electrical resistance. It cures and becomes thin layer after multiple hours in contact with oxygen. This process will be sped up using a heated build plate. PI-ETPU is a flexible thermoplastic that can also electrically conduct, however, its resistance is much higher than that of silverink. A combination of both silverink and PI-ETPU is used to ensure that in case the silverink breaks the PI-ETPU will still provide electrical connection.

Under the Octopus there is a PI-ETPU patch that acts as ground. The width of the band is dictated by the width of the three electrodes. The electrodes cannot be bigger since they would exceed the width of the biceps.

The Octopus is housed in a box made of Novamid ID 1070 (Novamid). This is a nylon filament with high strength and toughness. Two screws are used to attach the lid to the rest of the electronics box. They are screwed in from the underside and between the box and the X60, where the screws go in, a small plate of BVOH Water soluble filament (Fiberlogy) is printed. After the print, the BVOH can be dissolved in water and the corners of the X60 can be pulled apart to put the screws in.

The Novamid box, the two screw holes and the BVOH under the box can be seen in fig. 3.1.

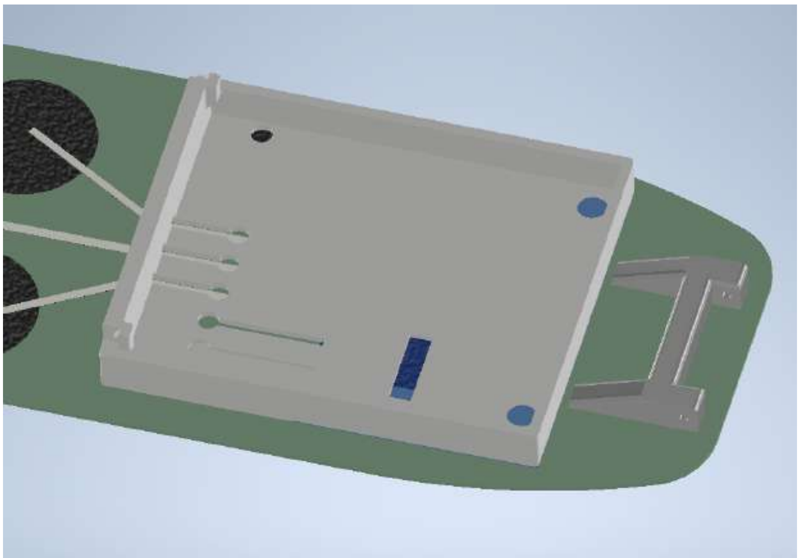

Figure 3.1: A detail of the band v1: the Novamid box (grey), X60 (green) and BVOH (blue).

The band on a subject's biceps can be seen in fig. 3.3. The three electrodes are visible on top of the muscle, while the electronics box is seen on the side of the arm.

Figure 3.2: The first complete prototype of the band.

Figure 3.3: The first prototype of the band on a subject's biceps.

3.1.2 sEMG band: version 2

Although the first version of the band works well, it can only detect activity from the biceps. For the second version 6 electrodes are used so that both the biceps and the triceps can be measured on. Because six electrodes take more space the watch band previously used can no longer be used. Only the metal clasp from a watch band is used this time. The backside of the band with the holes is now printed, instead of bought like for version one. This has the advantage that the band is more flexible so it can expand with the arm when the muscles are flexed. The previous version used a small BVOH plate to make the screw holes accessible. However, adding this plate makes the print more complex and it can cause warping since the Novamid does not attach well to the BVOH. Therefore it is decided to not include the plate. Instead, the 2 screw holes are made accessible by separating the X60 and Novamid with a knife after the print is finished.

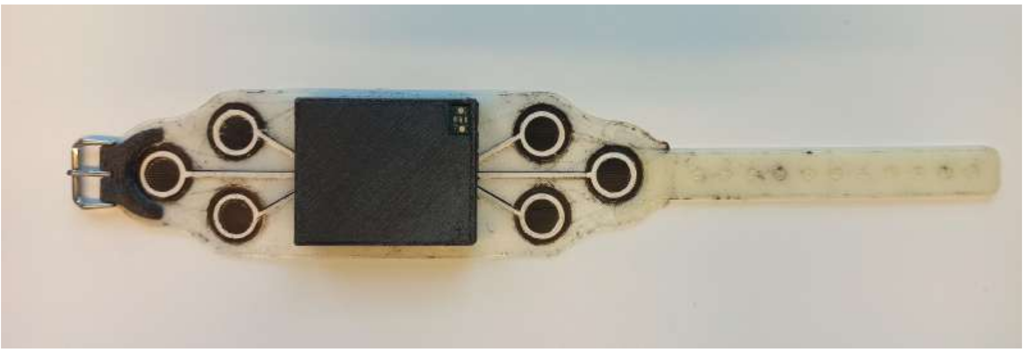

Figure 3.4: The second prototype of the band.

3.1.3 sEMG band: version 3

Version 3 is not much different from version 2. Version 2 had a small problem where the PI-ETPU did not fully connect, resulting in signal loss. This had been fixed in version 3. Also, the box with electronics has been rotated 90 degrees. This is to prevent electrodes from losing contact with the skin because of the box. This problem can be seen (very exaggerated) in fig. 3.5. Because the electronics box is not square, the situation improves when the box is rotated. Version 3 is visible in fig. 3.6.

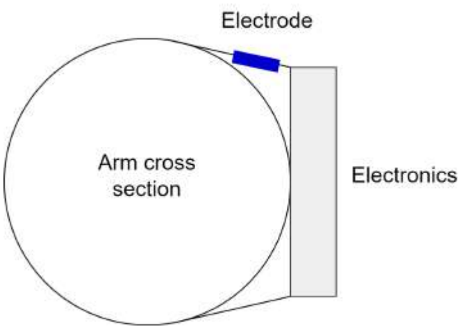

Figure 3.5: Electrode losing contact with the arm due to the electronics box.

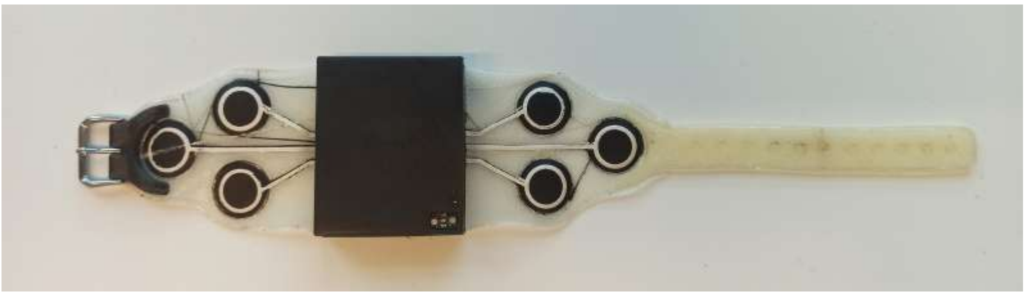

Figure 3.6: The third prototype of the band.

3.2 Limitations

The main limitations of this research are due to a time limit on the research. A selection has to be made on what variables are looked into, and which variables are not. For example, the electrode diameter and exact placement could be interesting subjects to look into, but due to limited time, this is not done. The materials chosen for the band are mainly the same as the ones from Martijn Schouten's band. If the research were longer, it would be interesting to look at different materials and evaluate their properties. For example, Novamid proved difficult to print at times, and a material like ABS could be sufficient to print the electronics box.

Another limitation is the lack of test subjects. The design variables and the different versions of the band have only been tested on one subject. Furthermore, they are not tested on actual Duchenne patients.

Since the Octopus (and its software) is used for all bands, this is also a limitation. Maybe the results of the tests could be improved by different electronics or different software.

3.3 Conclusion

In this section, it has been shown how the different prototypes came to be and what they look like. Although the third prototype does satisfy multiple requirements, it does not satisfy them all. This is because the third prototype is still a prototype and further development is needed to make a complete product. In the "Results and Discussion" chapter, the technical requirements will be discussed.

In table 3.1 the main differences between the different versions of the band can be seen.

Metric	**Version 1**	**Version 2**	**Version 3**	**Version 3.1**
Number of electrodes	3	6	6	6
Warping	No	No	Yes	No
BOVH plate	Yes	No	No	No
Orientation elec. box (horizontal/vertical)	H	H	H	V

Table 3.1: Main differences between the different versions of the band.

The technical details to produce the band can be found in the following chapter.

4 Fabrication

In this section, the technical details of the production of several test structures, as well as the prototypes of the band are discussed.

4.1 Fabrication process

All prints are designed in Autodesk Inventor and sliced using Ultimaker Cura. After exporting the G-code, they are printed using a Diabase Engineering H-series 3D printer. The heated nozzles are calibrated, so they have the same offset to the bed. This is done using a touch-off plate, and setting the Z value to zero. The full procedure can be found at the Diabase website [22]. Before a print all nozzles are primed, and by extruding a small length of filament it is made sure none of the nozzles are clogged. The X60 Ultra-Flexible Filament (COEX) is extremely flexible, and a length (1-2 meters) on the spool is lubricated with canola oil before printing to make sure the feeding will go smoothly. Finally, before printing the bed is cleaned with ethanol, and an adhesive spray is applied. In table 4.1 the used printing settings for different materials are listed.

4.2 Design variables

There are many variables in the fabrication process and design of the band that can be changed. Some important variables are:

- Electrode diameter
- Electrode infill
- Electrode protrusion
- Pressure on the electrode
- Electrode placement
- Closing mechanism
- Size adjusting mechanism
- Geometric properties

The electrode infill and the pressure on the electrode will be tested to see what the influence is of changing these parameters. The electrode diameter is chosen to be as large as possible while still fitting on the muscle because this is more favorable when dry electrodes are used [23]. The

Material	Temperature (degrees C)	Flow (%)	Print speed (mm/s)	Infill (%)	Fan speed (%)
X60 Ultra Flexible Filament (COEX)	215	125	20	70	100
PI-ETPU 85-700+ (Palmiga Innovations)	220	100	15	100	100
Novamid ID 1070 (Novamid)	285	85	15	100	100
BVOH water soluble filament (Fiberlogy)	210	100	60	100	100
Silverink CI-1036 (Engineered Materials Solutions Inc.)	Room temperature (no heating)	130	20	100	100

Table 4.1: Printing settings for different materials.

protrusion will not be tested, since when electrodes protrude from the band, this will result in a higher pressure, and the effects of pressure will be tested. The electrode placement, closing mechanism, size-adjusting mechanism, and geometric properties are dependent on the design and, thus, cannot be easily tested.

4.2.1 Infill

The first variable that is tested is the infill of the electrodes. To test the influence of the infill different electrodes, in groups of three, are printed, with varying infill. The following infill values are tested: 35, 45, 60, 75, 90, 100, and 110 percent infill. 110 percent infill is realized by setting the extrusion multiplier to 1.1. The electrodes are printed with a Diabase Engineering H-series 3D-printer and can be seen in fig. 4.1. Each trio also has the infill percentage printed on it, so no confusion can occur about what infill a trio is. The electrodes themselves are 20 mm in diameter, and made of PI-ETPU 85-700+ (Palmiga Innovations) they extrude 0.5 mm from the surrounding X60 Ultra-Flexible Filament (COEX). The extrusion is made possible by printing a layer of BVOH water-soluble filament (Fiberlogy) underneath the X60. This layer can later be removed by putting the print in water and letting the BVOH dissolve.

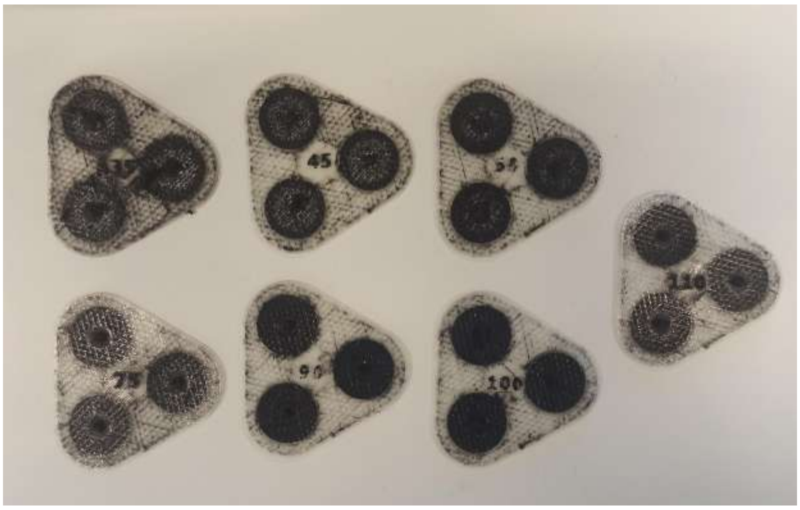

Figure 4.1: Groups of electrodes with different infill settings, ranging from 35 to 110 percent.

4.2.2 Silverink

It is also possible to print CI-1036 stretchable silver-ink (Engineered Conductive Materials), instead of PI-ETPU 85-700+ (Palmiga Innovations) as an electrical conductor. This is done using a Viscotec Viprohead 3 extruder with a 0.864 mm nozzle fixed to the Diabase printer. The pressure to the Viscotec is set at 1 bar. A result of using the Viscotec is that it is only able to use roughly one-third of the bed since it is not fixed in the middle of the printing area compared to the other nozzles. This greatly limits how big designs can be.

To explore what the differences are between using silverink and PI-ETPU, two test pieces are printed. Two electrodes will be pressed against the skin, and the electricity flows to two snap buttons that are attached via either PI-ETPU or silverink.

First, sEMG stickers are used for snap buttons, this can be seen in fig. 4.2. However, after testing the prints with a multimeter it was concluded that the sEMG stickers raise the resistance significantly, and therefore will distort the test results. Printing snap buttons like the ones in fig. 4.1 also proved very hard and yields unreliable results since the printer is unable to print such small buttons with sufficient accuracy. When they are successfully printed, they easily come loose from the connector. Another method is to attach the snap buttons using sil-

verepoxy, but this again raised the resistance of the electrodes significantly, and the connection is not very strong.
The final solution is to attach a metal snap button (normally used on clothing) directly to the electrode as seen in fig. 4.3. This has a number of advantages compared to the methods mentioned previously:

1. Attaching the buttons takes little time and is easy
2. The connection does not require curing for extended times or temperatures
3. The connection is very strong
4. The resistance is very low

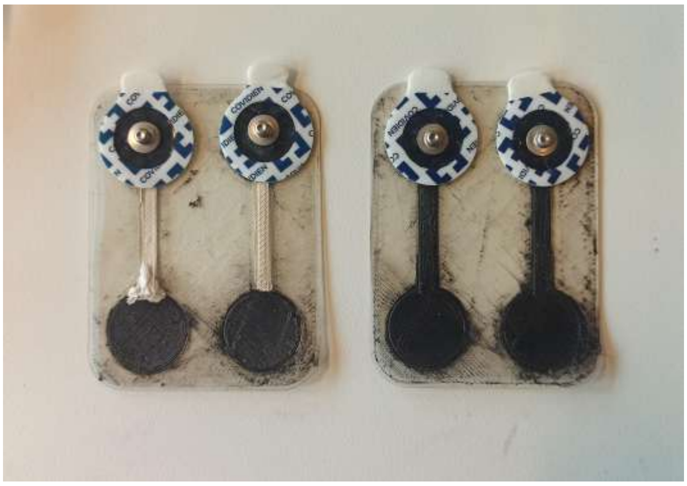

Figure 4.2: One electrode pair connected with silverink (left), one with PI-ETPU (right). Both use sEMG stickers.

Figure 4.3: An electrode with a snap button attached (left) and the corresponding connector (right).

The final printed electrode pairs, with metal snap buttons, can be seen in fig. 4.4. The electrodes are 20 mm in diameter, printed with 100 % infill, and kept together by X60 ultra-flexible filament. On the backside of the electrodes with the metal snap buttons, non-conductive tape is applied, so these electrodes cannot contact the skin directly. The print is printed on a heated bed at 75 °C, and afterward cured for 30 min at 100 °C to make sure the silverink is cured, and to lower the resistance of the PI-ETPU.

Figure 4.4: One electrode pair connected with silverink (left), one with PI-ETPU (right). Both use metal snap buttons.

4.3 sEMG bands

4.3.1 sEMG band: version 1

The first version of the band (fig. 3.2) uses a flexible rubber watch band with a metal clasp from an unknown supplier. The 3 electrodes with a diameter of 20 mm are made of PI-ETPU with an infill of 100 %. The flexible part of the band is made of X60 with 70 % infill, and the housing of the electronics, as well as the attachment points of the watch band, are made of Novamid ID 1070 (Novamid). The Novamid 1070 forms a sufficiently strong bond so additional glue is not required. The white lid of the electronics box is made out of PLA.

The band is printed on a heated bed of 75 °C, and after printing cured in an oven at 100 °C for 30 min to make sure the silverink is cured, and to lower the resistance of the PI-ETPU.

4.3.2 sEMG band: version 2

The second prototype of the band is visible in fig. 3.4. It has six 20 mm electrodes, again made out of PI-ETPU. The flexible, translucent part is made from X60 with an infill of 70 %. The box for the electronics, the lid, and the clasp attachment point are made of Novamid 1070 with an infill of 100 %. The band is printed on a heated bed of 75 °C, and after printing cured in an oven at 100 °C for 30 min to make sure the silverink is cured, and to lower the resistance of the PI-ETPU. The metal clasp is taken out of a wristband for a Galaxy watch 46 mm (Aliexpress).

4.3.3 sEMG band: version 3

Version 3 is made with the same materials, infill, bed temperature, curing time, and temperature as version 2, except for the PI-ETPU. Instead of PI-ETPU 85-700+, PI-ETPU 95-250 was mistakenly used.

A problem that happened with this version is the warping of the Novamid box. The warping is so extreme, that the Octopus no longer fits inside, see fig. 4.5. This might be a result of the rotated box. With this version, the box is no longer surrounded on all sides with X60, which acts as an adhesive between the bed and the Novamid. Without the X60 on two sides, the Novamid box warps.

Figure 4.5: An example of the electronics box warping.

4.3.4 sEMG bands: version 3.1

Version 3.1 was created to fix the problems from version 3. Here, the correct filament PI-ETPU 85-700+ instead of PI-ETPU 95-250 is used. Also to counteract the problem of the warping electronics box, a brim (fig. 4.7) of X60 is printed around the box. This brim can be removed with scissors after printing and prevents the Novamid from warping.

The pressure put on the Viscotec is raised from 1 bar to 3 bar. This is because the nozzle gets clogged regularly during printing, and this results in incomplete silverink traces (fig. 4.6).

Figure 4.6: The result of a clogged Viscotec nozzle.

Other than the described changes, the settings, methods, and materials used in this version are the same as in version 3.

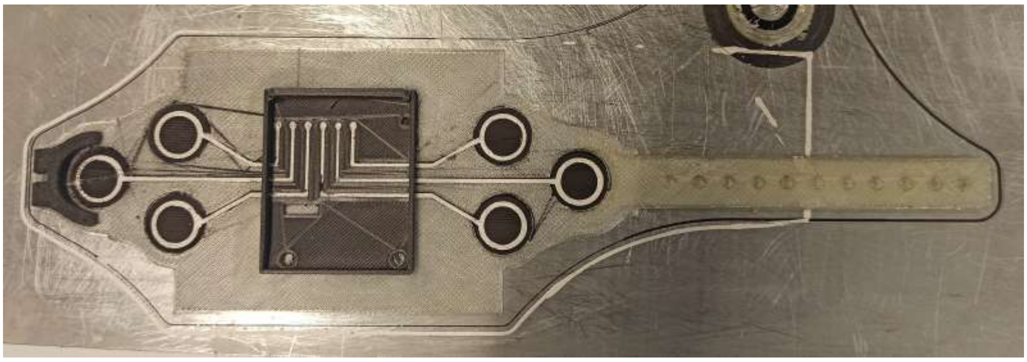

Figure 4.7: The band with its brim to prevent warping.

4.4 Conclusion

In this chapter, the necessary parameters, details, and materials to make the band are listed. Also, it is concluded that using metal snap buttons is the best way to attach 3d printed structures to a wire. In the case of under extrusion by the Viscotec, a solution is to increase the pressure. Finally, to prevent the warping of Novamid, a brim of X60 is printed around the band.

5 Measurements

In this chapter the measurements that the designs, listed in chapter chapter 3 and printed using settings and materials detailed in chapter chapter 4, are described. This is done so the effect from certain parameters (infill, silverink or PI-ETPU, pressure on the electrode) can be evaluated. Also, measurement setups are described for the different versions of the band, so the bands can be compared, and evaluated according to the requirements.

For the measurements described in this chapter, the sampling rate of the Octopus is set at 1000 samples per second, with a lead-off current of 24 nA, thus all properties are evaluated in a bandwidth up to 500 Hz. To calculate the impedance a current is send through the electrodes at a quarter of the sampling frequency. An algorithm is then used to calculate the impedance. Further information about signal processing can be found in the conference paper attached in the appendix.

For each experiment, the standard deviation is calculated. It is normalized by N-1, where N stands for the number of data points. When the signal-to-noise ratio is calculated, it is done by creating a ratio in decibels of the signal (where the muscles are contracted) compared to the noise (where the muscles are relaxed).

5.1 Experiments

Below are various exercises, used to evaluate the performance of the prints. In table 5.1, it can be seen which exercise is used to measure the performance in what experiment. The details of each exercise can be found in section 5.1.1 to section 5.1.3.

5.1.1 Exercise 1: Isometric and isotonic contractions of the biceps

- Sit in a chair, with the underarm resting on a table, under a 90-degree angle with the upper arm.
- Flex the biceps, up to the point the hand is almost starting to lose contact with the table. This should take roughly 2 seconds in total.
- Slowly relax the biceps again, this should also take 2 seconds.
- Redo the last 2 steps 2 times, so a total of 3 times flexing and relaxing the biceps.

Followed by isotonic exercises:

Table 5.1: Different experiments and their corresponding exercises.

Experiment	Exercise 1	Exercise 2	Exercise 3	Exercise 4
Infill	X			
Silverink		X		
Pressure (Inflatable armband)	X			
Pressure (Blood pressure meter)		X		
sEMG band: v1		X		
sEMG band: v2		X		
sEMG band: v3			X	
sEMG band: v3.1			X	X

- Sit in a chair, with the arm resting on a table, under a 45-degree angle.
- Flex the biceps and slowly lift the lower arm off the table until it reaches a 90-degree angle with the table. This should take roughly 5 seconds in total.
- Slowly let the lower arm down again, until it lays flat on the table. This should also take 5 seconds to do.
- Redo the last 2 steps 2 times, so a total of 3 times raising and lowering the arm.

5.1.2 Exercise 2: Isometric contraction of the biceps

- Sit in a chair, with the underarm resting under a table on the upper leg, under a 90-degree angle with the upper arm. The muscles of the arm should be fully relaxed.
- Push the arm against the underside of the table and keep it there for 1 second.
- Relax the arm again

5.1.3 Exercise 3: Isometric contractions of biceps and triceps

- Sit in a chair, with the arm resting on the table, so that the upper arm makes a 90-degree angle with the table
- Relax the arm fully
- Flex the biceps for 2 seconds and make sure the arm does not leave the table. This can be prevented using the other arm
- Fully relax the arm again, for 2 seconds
- Flex the triceps for 2 seconds
- Relax the arm fully

5.1.4 Exercise 4: Isotonic contrations in force setup

- Sit in a chair, grab the handle of the setup and relax the upper arm muscles. Make sure that the elbow is at the center of rotation.
- Slowly raise the lower arm, until an angle of roughly 50 degrees is achieved.
- Lower the arm until its back at the 0-degree angle.
- Repeat the first three steps.

5.2 Design variables

5.2.1 Infill

To evaluate what the effect of the infill is on the impedance and the EMG envelope, the test listed in table 5.1 is done. The electrode groups from fig. 4.1 are put under a sweatband on the biceps. They are connected with wires using snap buttons to the Octopus.

5.2.2 Silverink

In order to test the effects of using silverink on the impedance, the signal-to-noise ratio and the phase of the printed electrodes (fig. 4.4) will be put under a sweatband, so that the pressure with which the electrodes are pushed against the skin will be the same. Then the test from table 5.1 will be performed.

25 exercises are done in total for each pair, between each 5 the electrodes are slightly moved to average out the difference between positions and make sure build-up moisture under the electrodes will not influence the results.

5.2.3 Pressure on the electrode using inflatable armbands

To test the effect of electrode pressure on the EMG envelope, the impedance, the SNR, and the phase, an inflatable armband made by Intex (commonly used by people to stay afloat in a pool) will be used. The electrodes (the left pair in fig. 4.4) are put between the skin and the armband so that the armband pushes the electrodes against the skin. The armband can be easily inflated, thus increasing the pressure on the electrode. Each time the band is inflated a bit more, five isotonic exercises are performed as described in section 5.2.1.

It is not possible to do an absolute test, since using an inflatable armband does not yield a metric for the pressure. However, it is possible to do a relative test since it is known the pressure increases between each measurement. Therefore, it is made sure that the electrodes do not move between exercises, to minimize the variation this causes.

Figure 5.1: Inflatable armbands, also known as floaties. Image source: [24].

5.2.4 Pressure on the electrode using a blood pressure meter

The method with the inflatable armband is not very accurate, since it is not possible to measure the pressure. Therefore, a sphygmomanometer (commonly known as a manual blood pressure meter) is used. (visible in fig. 5.2). When the electrodes (the left pair visible in fig. 4.4) are put under the inflatable part of the blood pressure meter (left side of fig. 5.2), the pressure with which the band pushes the electrode against the skin can be precisely read from the gauge. This time, isometric exercises (as described in section 5.2.2) are used, since the band is rather big, and isotonic exercises disturb the position of the band. Five exercises are performed at each of the seven pressure levels.

Figure 5.2: A sphygmomanometer in use. Image source: [21].

5.3 sEMG bands

5.3.1 Requirement evaluation

Since the band is still in the prototype stage, not all requirements are evaluated. Only the requirements below will be evaluated with the methods described below it for all bands, but only on one test subject. They are the same as the requirements in table 2.1, but are repeated here for the reader's convenience.

- T1: Transmit good quality sEMG signal
  Make sure the SNR is at least a ratio of 10 (20 dB)
- T2: Achieve constant quality sEMG signals
  Make sure the impedance standard deviation is less than 5 %
- T3: Be rechargable
  Check if there is a possibility to recharge the battery
- T4: Can function for an extended time
  Turn the device on, and measure the time (at least 4 hours) before the band stops working
- S1: No sharp edges on the band
  Run a finger carefully along all edges of the band and feel if they are sharp
- U1: Be easy to put on or take off by a different person
  The subject will test this one on themselves, they should be able to put on the band from it laying on a table within one minute
- U2: Be adjustable for different arm sizes
  It can be verified whether the band is adjustable, but not on different test subjects
- U4: Be comfortable to wear for the patient
  Wear the band for 10 minutes, and describe if it is at least a 7/10 comfortable
- U6: The band should be reusable
  Check that the band works for two sessions of thirty minutes

5.3.2 sEMG band: version 1

To evaluate the performance of the first version of the band isometric exercises, like described in table 5.1, are performed. The band is positioned so that the electrodes are on top of the biceps, like visible in fig. 3.3. In total 25 exercises are done, between every five exercises the band is slightly moved to create an average and minimize the role of the position of the band.

5.3.3 sEMG band: version 2

The second version of the band was tested as described in table 5.1, so using exercise 3. Also for this band, the electrical resistance was measured at the bottom of the electrodes by using a multimeter. A total of three resistance measurements were done per electrode, by holding one probe in the middle of the electrode, and the other one near the edge. The resulting resistance was read after resting the probes on the electrodes for 3 seconds.

5.3.4 sEMG band: version 3

Version 3 of the band was tested using the test from table 5.1. This is a different test compared to the previous versions of the band, since now both the triceps and biceps need to be contracted, instead of only the biceps.

This exercise is done a total of five times, and the sEMG envelope and impedance are recorded. The resistance was also measured, in the same way as described for band version 2.

5.3.5 sEMG band: version 3.1

Version 3.1 was tested in the same way as version 3.

The band was also tested in an experimental setup that was made by Martijn Schouten. The setup can be seen in fig. 5.3 and fig. 5.4. It consists of an arm that can be rotated 90 degrees, and a TiePie oscilloscope to record the data. When rotating the arm, the force being put on it, and the angle of the arm is recorded. With this setup, exercise 4 is done.

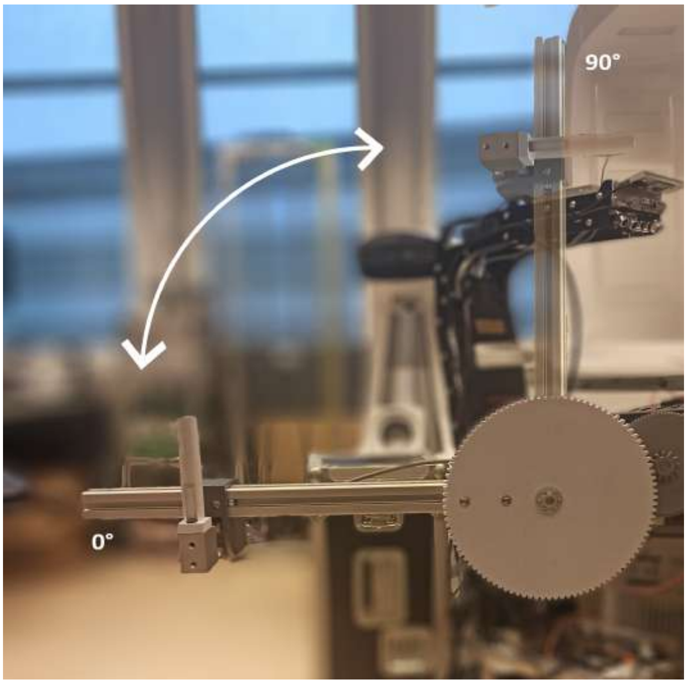

Figure 5.3: The force setup, and its range of motion.

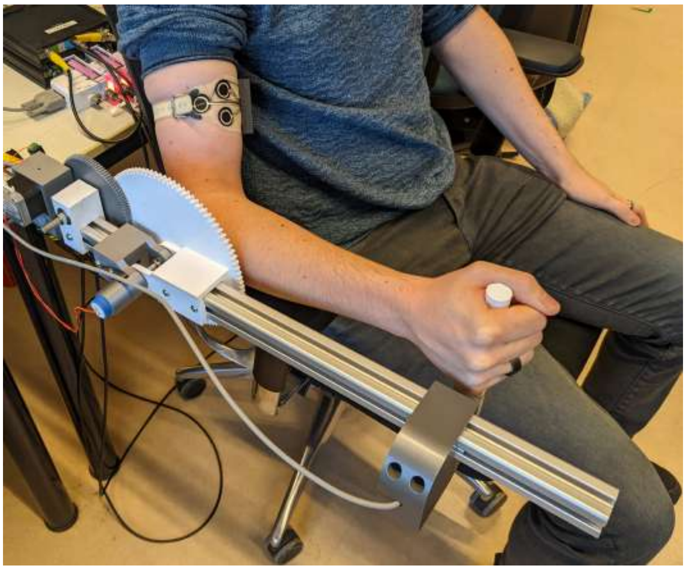

Figure 5.4: A test subject sitting in the force setup, with the sEMG band version 3.1 on his upper arm.

5.3.6 Using the band as a control system

Martijn Schouten has developed a game to test the band's capability as a control system. In this game, a red square is visible, which travels on a vertical line in a seemingly random pattern. A green square sits still in the middle of the same vertical line and can be moved up by contracting the biceps, and moved down by contracting the triceps.

The goal of the game is to follow the red square by moving the green square using the biceps and triceps. The sEMG envelope from sEMG band is used to do this. First, a maximum contraction is set at a value of 1 for the biceps, and -1 for the triceps. The values from the sEMG envelope are then scaled with a factor of 200 to convert them to pixels on the screen.

The game will run for a total of two minutes, and the position of the red and green square during this time will be saved. Band version 3.1 will be used for this.

Similarly to the square game, the sEMG signal of the band can also be used to control other games. Now when the integrated sEMG envelope is above a threshold, contracting the biceps moves the cursor of the computer to the left, and contracting the triceps moves it to the right. When the muscles are relaxed, the cursor stays where it is. Maximum boundaries are set for the cursor, so it cannot be moved outside the game window.

5.4 Conclusion

In this chapter four different exercises, as well as controlling game input are described that are used to measure the performance of the test structures and the different bands. In the next chapter, the resulting metrics from these tests will be discussed.

6 Results and Discussion

In this chapter, the results of the measurements that are described in chapter 5 are displayed and discussed.

6.1 Design variables

6.1.1 Infill

The impedance and its standard deviation for different infill settings can be seen in fig. 6.1. It can be seen that the standard deviation does not change much at 60 % infill or higher. This can also be seen in fig. 6.2, where the flexing and relaxing of the biceps can be seen in the form of three peaks. As can be seen, the signal from 60 % infill is very similar to the signal from 100 % infill. In the graph at 100 percent infill, the sEMG envelope did not go back to zero. This is most likely because the test subject did not fully relax his muscles.

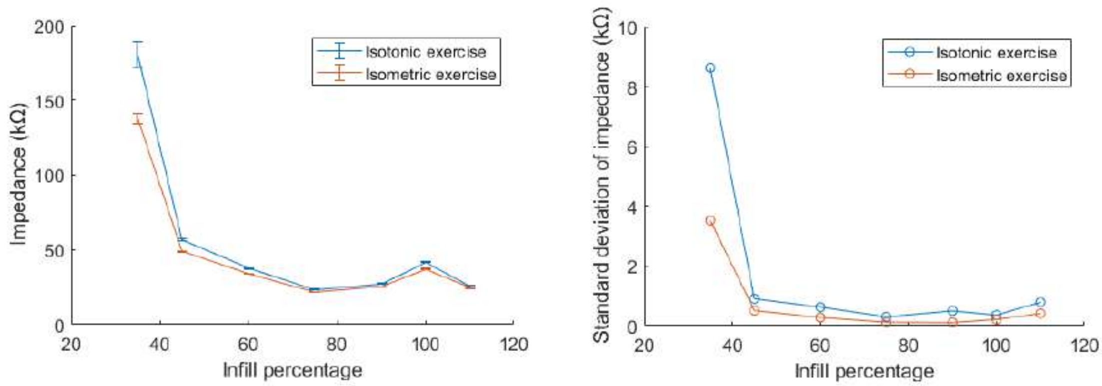

Figure 6.1: The absolute value and standard deviation of the impedance, at different infill values during both isotonic and isometric exercises, at 500 Hz. The standard deviation is also visible in the form of error bars on in the left graph.

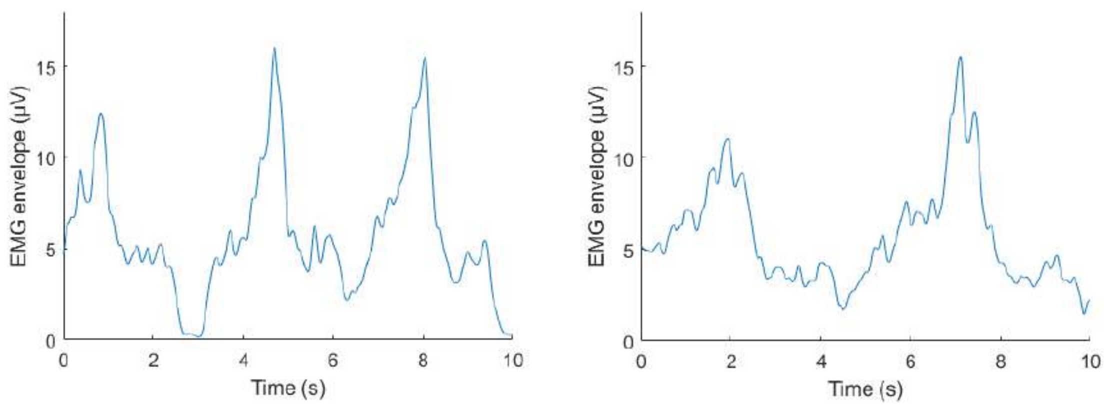

Figure 6.2: The sEMG envelope from isotonic exercises at 60 (left) and 100 percent infill. (right)

6.1.2 Silverink

In fig. 6.3 the sEMG envelope during the tests is visible when using PI-ETPU or silverink. Not only are the peaks higher when using silverink, the noise between peaks is also lower.

The resulting impedance, the standard deviation of the impedance, phase and SNR of the tests are given in table table 6.1. It can be seen that using silverink lowers the absolute value of the impedance, and lowers the standard deviation. It also raises the signal-to-noise ratio, and lowers the phase. This is in line with expectations since the electrical resistance of silverink is much lower than that of PI-ETPU.

Metric	Unit	Silverink	PI-ETPU
Impedance	KOhm	65.77	473.81
St. dev. of impedance	KOhm	2.39	11.40
Signal to noise ratio	dB	14.94	10.26
Phase	degrees	-52.62	-8.52

Table 6.1: Differences between using the silverink trace and the PI-ETPU during isotonic exercises at 500 Hz.

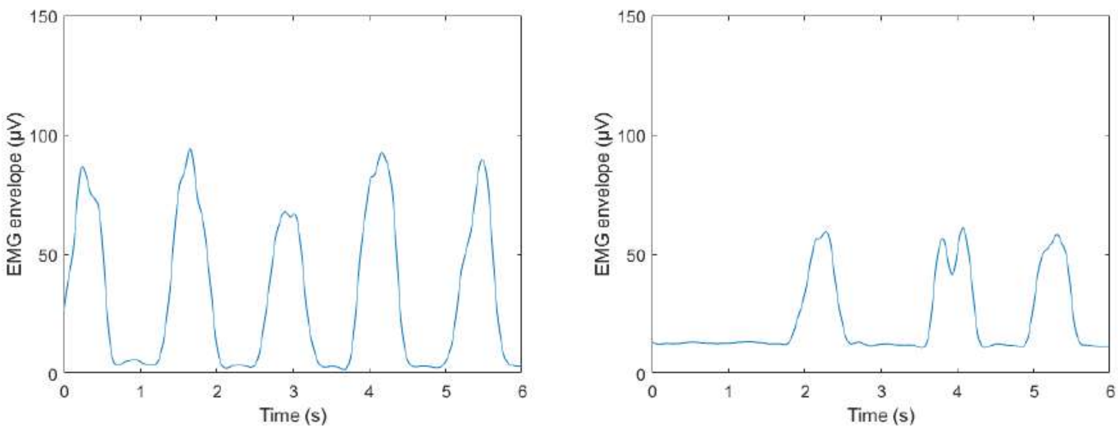

Figure 6.3: The sEMG envelope when using silverink (left) and PI-ETPU (right) during isometric exercises.

6.1.3 Pressure on the electrode using inflatable armbands

The signal at the highest and lowest pressures can be seen in fig. 6.4. It should be noted that in the lowest pressure graph, the 5 exercises can still be easily seen. The noise when there is no signal, however, is much higher. The resulting signal-to-noise ratios and phase can be seen in fig. 6.6. The impedance and standard deviation of it across different pressures are visible in fig. 6.5. As can be seen, the impedance and standard deviation of the impedance go down with increasing pressure, while SNR goes up, and the phase does not change much. These changes would indicate that higher pressures give better results.

It should be noted that in figs. 6.4 to 6.6 there is no value or unit for the pressure since this is not possible to measure using only an inflatable armband. However, these measurements do give a rough idea of what increasing pressure does to these variables. A better test is needed to more accurately verify the effect of pressure on the electrode.

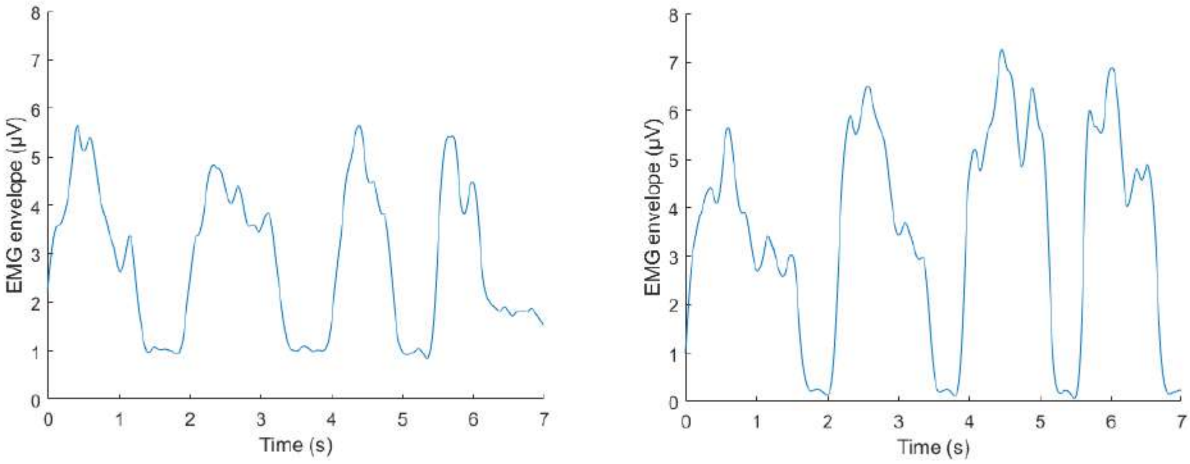

Figure 6.4: The lowest (left), and highest pressure (right) on the electrode, with 4 isotonic exercises visible.

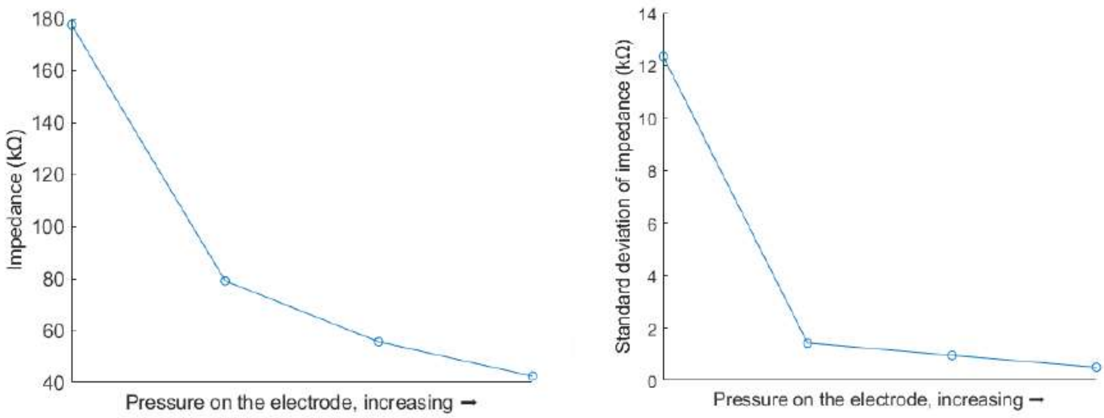

Figure 6.5: The standard deviation and absolute value of the impedance for different pressures on the electrode during isotonic exercises, measured at 500 Hz.

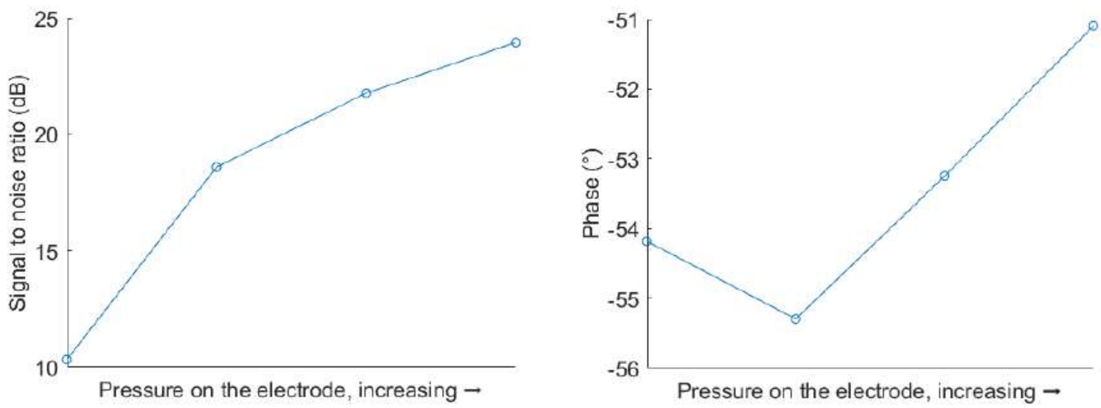

Figure 6.6: The signal-to-noise ratio and phase for different pressures on the electrode during isotonic exercises.

6.1.4 Pressure on the electrode using a blood pressure meter

Like the tests with the inflatable armband, a look is taken at the impedance, the standard deviation of the impedance, the phase, and the signal-to-noise ratio. These variables can be seen in fig. 6.7 and fig. 6.8. It can be seen that the impedance and the standard deviation of the impedance both go down significantly with increasing pressure. This is in line with the expectations, and the results from the inflatable armband experiments. However, this does not necessarily result in a higher signal-to-noise ratio. As can be seen in fig. 6.8, a trend line going upwards can be drawn. However, if the first data point is ignored, (this is not enough pressure to keep the band on the skin), the trend line becomes almost horizontal. The phase also barely changes with increasing pressure.

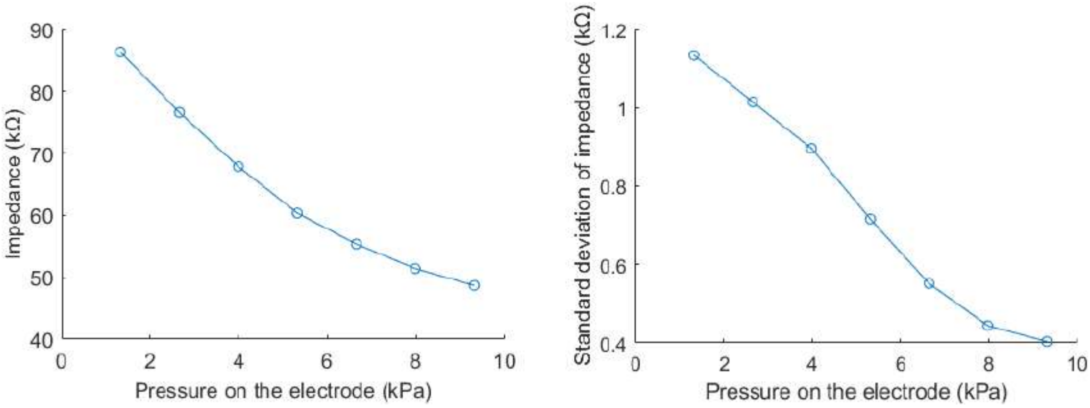

Figure 6.7: The standard deviation and absolute value of the impedance for different pressures on the electrode during isometric exercises, measured at 500 Hz

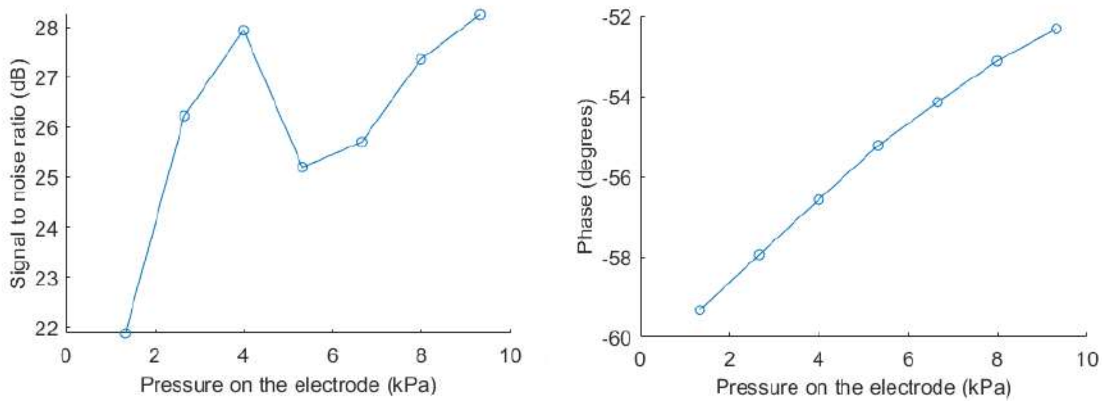

Figure 6.8: The signal-to-noise ratio and phase for different pressures on the electrode, during isometric exercises.

6.2 sEMG bands

6.2.1 sEMG band: version 1

In fig. 6.9 below the envelope of the sEMG signal can be seen. In table table 6.2 different metrics of the band are listed. As can be seen, the impedance is quite low, the standard deviation of the impedance is very low, and the SNR is high. These numbers result in a good signal, as can be seen in fig. 6.9.

When evaluating the requirements from chapter 5 it can be seen from table 6.2 that requirements T1 and T2 are met. The band is also rechargeable (T3) but does not work for 4 hours (T4), since the Octopus shuts off after a certain time.

From the safety requirements, only requirement S1 can be confirmed, since there are no sharp edges. The subject was able to put on a band within one minute and the band is adjustable (U1 and U2). The subject described the band as a 7/10 comfortable, so this just passes (U4). Finally, the band is confirmed to work for two thirty-minute sessions (U6).

Metric	**Unit**	**Value**
Impedance	KOhm	20.35
St. dev. of impedance	KOhm	0.34
Signal to noise ratio	dB	35.6
Phase	degrees	-38.47

Table 6.2: Different average metrics of the sEMG band (first version) at 500 Hz

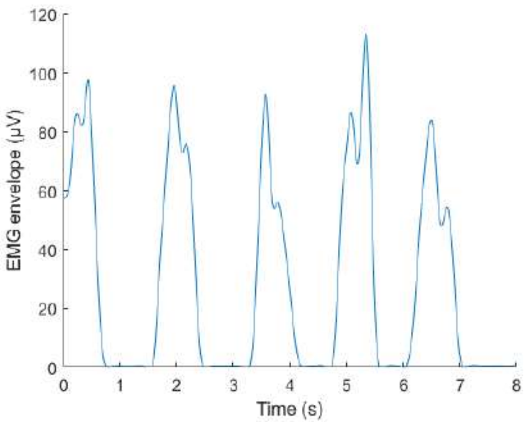

Figure 6.9: The sEMG envelope of the band when performing isometric exercises.

6.2.2 sEMG band: version 2

The sEMG envelope and raw EMG signal for the biceps using band version 2 can be seen in fig. 6.10. It is clear that something went wrong, as can be seen by the extremely high peaks. This is caused by electrodes losing contact. This is partly due to a design flaw in the band. In the design, there was a small gap (+- 0.1mm) between two PI-ETPU traces and the electrodes. Although the silverink was printed correctly on top, when stretching the band the silverink will develop small cracks, and thus also lose contact. This problem stresses the importance of putting PI-ETPU traces under the silverink.

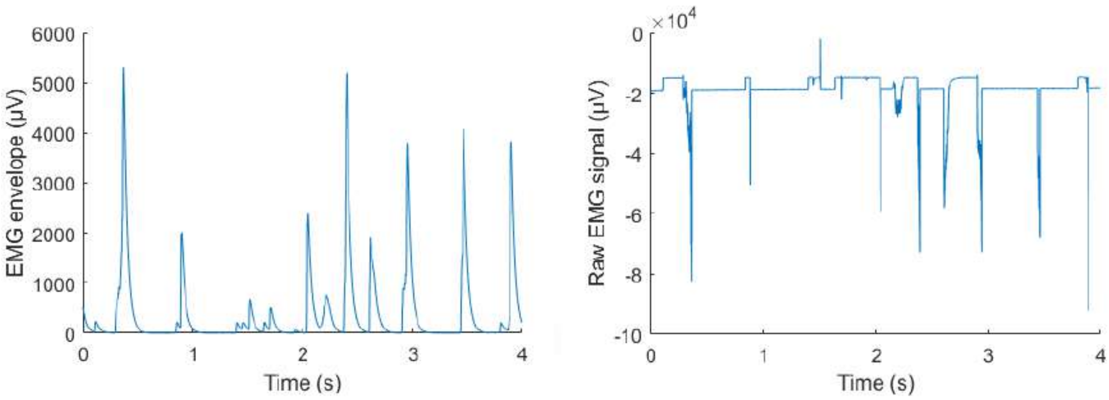

Figure 6.10: The sEMG envelope, and raw signal of the band when performing isometric exercises.

6.2.3 sEMG band: version 3

Resistance problems

Version 3 of the band did not produce a good signal, because the electrical resistance was very high. The resistance is compared to the resistance of the electrodes of version 2 of the band, and is visible in table 6.3. One of the reasons this happened is probably that PI-ETPU 95-250 was used, instead of PI-ETPU 85-700+. The former has a lower conductivity. Another reason could be that the failing electrodes are printed much closer to the bed. This results in a different texture, and this can be seen in fig. 6.11. PI-ETPU might have a much lower conductivity if the material is subjected to stress, which happens when the nozzle is too close to the build plate.

Metric	**Unit**	**V2 (working)**	**V3 (not working)**
Resistance	KOhm	38.29	1633.03
St. dev. of resistance	KOhm	17.43	2046.13
Data points		9	9

Table 6.3: Difference in resistance between v2 and v3 of the band.

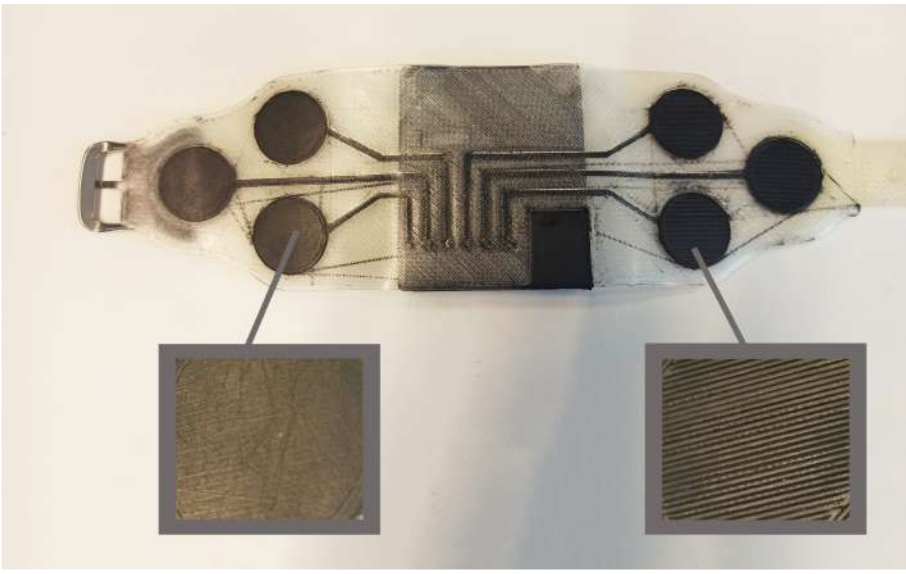

Figure 6.11: The structure on the underside of the electrodes.

6.2.4 sEMG band: version 3.1

Version 3.1 of the band was tested according to table 5.1, using exercise 3. So first, the biceps were contracted (first peak in the graph), and then after two seconds of rest, the triceps (second peak in the graph). The resulting EMG envelope is visible in fig. 6.12 in the left graph. Here two data sets are plotted. The blue signal is the envelope signal from the electrodes on the triceps, the orange signal is from the electrodes on the biceps. For both muscle groups the average signal is subtracted from the envelope. So for the biceps envelope, the average biceps signal is subtracted. As seen in the figure, there are two distinct peaks and there is barely any overlap. The peak from the biceps is higher than the one from the triceps, this is consistent across experiments. In the right graph, a triceps signal can be seen. In this particular experiment, there is some overlap. When the biceps are contracted, the triceps electrodes also pick some signal.

There could be different reasons for this. One reason could be that the electrodes are too big, and therefore picking up the signal from the other muscle. Another reason could be co-contraction, where both muscles were used instead of only one. Finally, the ground was placed under the box, so in between the muscles. This is very close to either muscle group, and it could pick up a signal.

Some other metrics of version 3.1 can be seen in table 6.4. Compared to version 1 the impedance and its standard deviation are roughly doubled. The signal-to-noise ratio, as well as the phase, is also quite a bit lower. It is unclear why this is the case. An explanation could be that the two electrode clusters are interfering with one another, or that the ground is not interfacing well with the skin.

Prototype version 3.1 also has some minor mechanical flaws. The ground, made from PI-ETPU, does not have a strong attachment to the Novamid box. These two materials will sometimes detach, resulting in a loss of signal. This could be improved by making sure there is X60 around the outlines of the Novamid box. This problem was temporarily solved by applying Loctite SF 770 primer and Loctite 406 super glue between de PI-ETPU and Novamid. The Novamid electronics box itself also does not fully close at times. On one side it closes with hooks, and with screws on the other side. The hooks do not work as a reliable method to keep the box closed, and a redesign of the box would be beneficial.

Also, this version is tested to see if it will satisfy the requirements from chapter 5. Requirements T1 and T2 can be verified from table 6.4. The outcome of the other tests remains the same as version 1, so all are passed, except the requirement "Can function for an extended time" (T4).

Metric	**Unit**	**Value**
Impedance	KOhm	42.50
St. dev. of impedance	KOhm	0.86
Signal to noise ratio	dB	26.49
Phase	degrees	-57.96

Table 6.4: Different average metrics of the sEMG band (version 3.1) at 500 Hz.

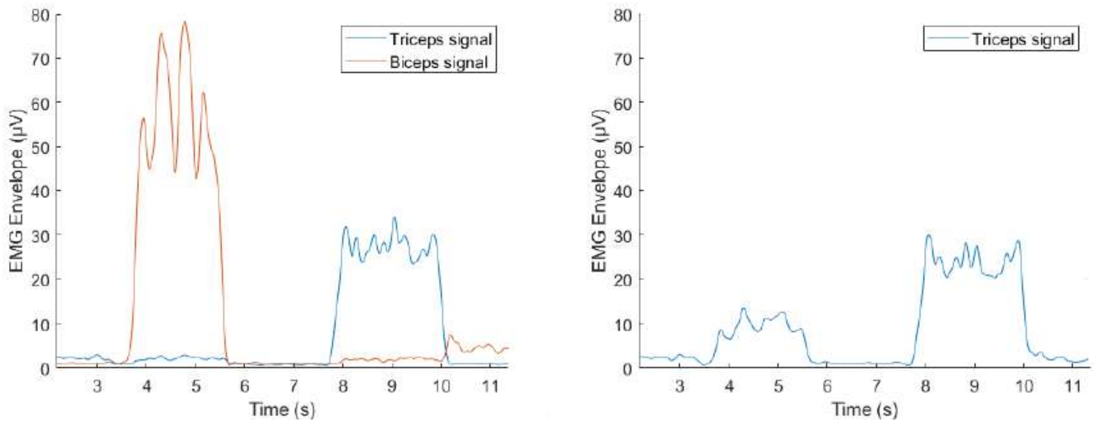

Figure 6.12: The sEMG envelope when performing exercise 4 (first contracting the biceps, then the triceps) for both electrode clusters (left), and only a triceps cluster (right). In the right graph, co-contraction can be observed.

This version of the band is also tested in the force setup from fig. 5.3 and fig. 5.4. The resulting angle of the lower arm, the force exerted by the arm, and sEMG envelope, can be seen in fig. 6.13 and fig. 6.14. It should be noted that when the arm-force is negative, the underarm goes up, and vice versa. An interesting effect is that the triceps signal has a very small amplitude compared to the biceps. This could be due to multiple reasons. First, the exercise might not be suitable for using both muscles. Another explanation could be that the electrodes on the triceps are not in the correct location, thus picking up a weaker signal.

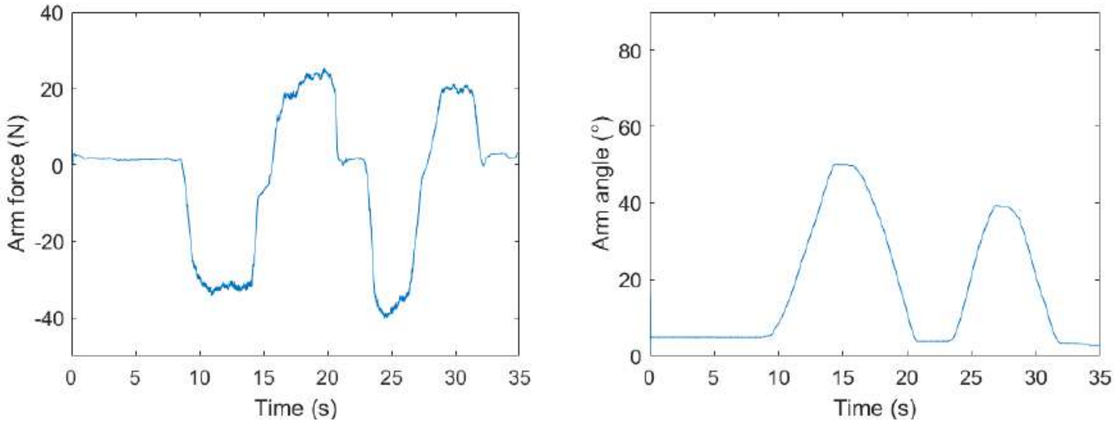

Figure 6.13: The force (left) and angle (right) of the arm when raising and lowering the lower arm.

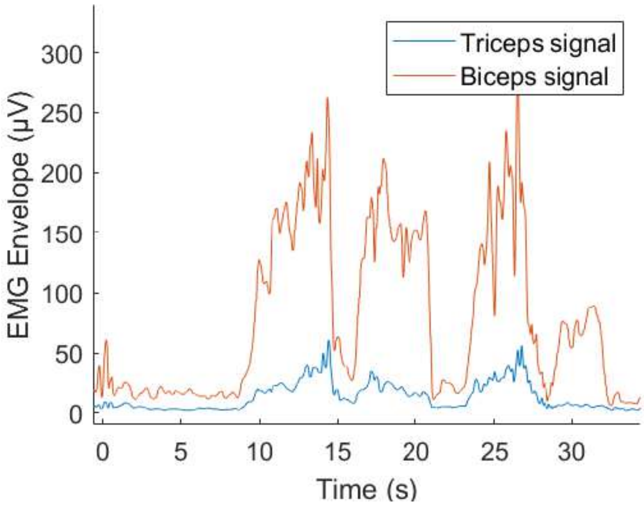

Figure 6.14: The sEMG envelope when raising and lowering the lower arm in the force setup.

6.3 Using the band as a control system

In fig. 6.15 both the red square that the user has to follow (orange line), and the green square that the user can control (blue line) can be seen. Thirty seconds of the two-minute experiment are shown. The y-axis represents the position on the screen, in pixels. In the left graph the unfiltered signal, made from the sEMG envelope, can be seen, while on the user input in the graph on the right a Butterworth filter is applied afterward. It can be seen that the blue line follows the orange line, thus confirming that the band can be used as a control system. The root mean squared error between the two lines is 116.49. It is unclear how much of the differences in the two lines are due to human error and reaction time, and how much is due to the software or band.

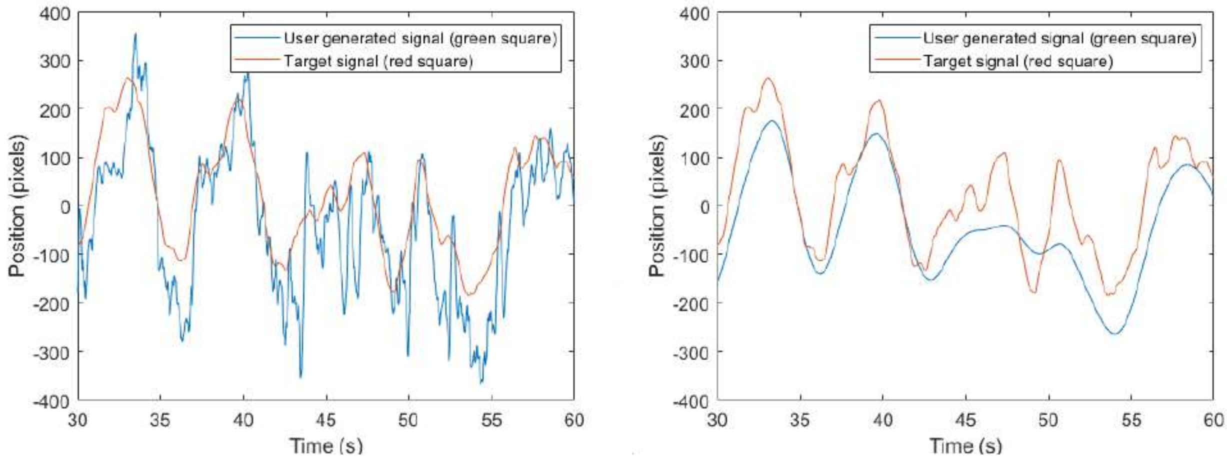

Figure 6.15: The position of the red and green square on the screen, unfiltered (left), and after using a Butterworth filter (right).

In fig. 6.16, the position of the two squares is again displayed. This time the user-generated signal is integrated in real-time. The root mean squared error between the two graphs is 44.65. The difference in RMSE can be seen in fig. 6.17. Due to this being significantly lower than the results from fig. 6.15, it can be said that integrating is preferred.

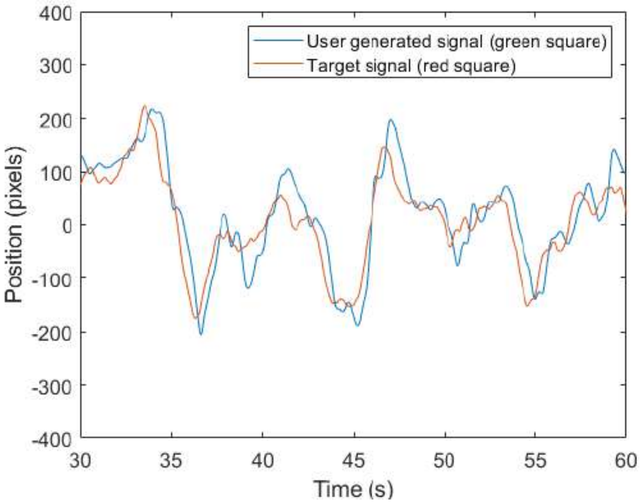

Figure 6.16: The position of the red and green square on the screen, the sEMG envelope input is integrated.

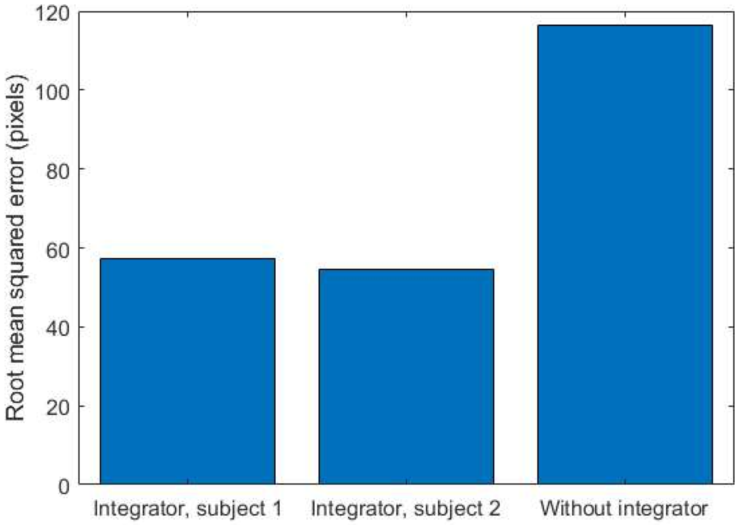

Figure 6.17: The difference in the root mean squared error of the in- and output of the square game between using an integrator and not using one.

The blue lines follow the orange ones with a delay. To calculate this delay, the user-generated signal is slightly shifted on the x-axis, and for each step, the root mean squared error between the two lines is calculated. It is found that the lowest mean difference occurs if the test subject were to be 0.42 s faster. The RMSE at different intervals can be see in fig. 6.18.

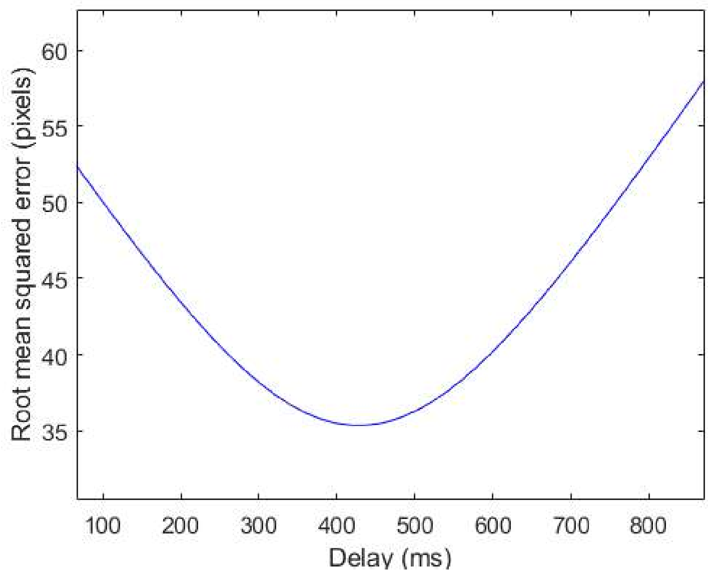

Figure 6.18: The root mean squared error of the in- and output of the square game at different delay values.

The average human reaction time for simple tasks is 0.22 s [19]. Because the reaction time in this experiment is 0.42 s, it can be concluded that the amount of delay the electronics and software add is comparable to the human reaction time.

In fig. 6.19 on the right, a QR code is visible which leads to a video that shows a test subject playing the game. The video can also be accessed by clicking here. The output of the band can also be used to move the cursor on a computer. Contracting the biceps will move the cursor to the left side, and contracting the triceps moves it to the right. This input can then be used to play games. The QR code on the left in fig. 6.19 leads to a video showing a test subject playing two games. The video can also be accessed by clicking here. Controlling the bubble shooter games shows that the test subject has good control of the arrow since they are able to match the colors of the bubbles quickly.

Figure 6.19: A QR code to access the video showing a test subject playing the red and green ball game (right) and using input from the band to play Galaga and Bubble Blaster (left).

6.4 Conclusion

In this chapter the findings, from the measurements explained in chapter 5, are displayed and discussed. The metrics from the band version 1 and 3.1 are listed, and the reasons why band version 2 and 3 did not work are discussed. Finally it is shown that the band version 3.1 can be accurately used a control system. In the next chapter conclusions from the research as a whole will be drawn.

7 Conclusion

A 3d printed sEMG band has been successfully designed and manufactured. It has been shown that, together with the Octopus sEMG amplifier, it can be successfully used for game control, thus opening the way for using the band for controlling an exoskeleton.

From the infill experiments, it can be seen that the impedance and its standard deviation do not change much if the infill is 60 % or higher. Therefore this variable is not a deciding factor in the design of the bands. Any infill value or 60 % or higher is sufficient.

From the test comparing silverink and PI-ETPU, the results show that using silverink will lower the impedance, its variation, and the phase, and raise the signal-to-noise ratio. Because these are all desired changes, it can be concluded that silverink is preferred when using it as a conductor.

However, silverink is also very fragile, and this can be seen from the failure of band version 2, where there was no PI-ETPU under a very small section of the silverink, resulting in a signal loss. Combining these two findings means it is beneficial to use PI-ETPU with silverink on top to conduct electricity whenever applicable.

Both tests in which pressure was put on the electrode lead to the same conclusions. Although the impedance and its standard deviation decrease with increased pressure, the SNR and phase do not change significantly as long as the pressure is above a minimum value to keep the electrodes pushed against the skin. So, the pressure is not a deciding factor in making a good signal.

Band version 3 did not work, it is suspected that this is partly due to a nozzle that is too close to the bed, therefore subjecting the PI-ETPU to too much stress, resulting in it having a very high resistance. This is a theory, and it would be interesting to confirm or debunk this with experiments.

When looking back at the requirements from table 2.1, it should be noted that this list is for a finished product. However, the band is still in the prototype phase, and the most recent version 3.1 does not satisfy all requirements. This is in part due to not all requirements being tested, since some could lead to severe damage to the band or the electronics.

But this table does dictate how the development of the band could go in the future, and what tests still need to be done before the band can be considered "completed".

The tests with the square game, and the two other games, prove that the band can be used as a control system, with good accuracy and speed. However, this is only tested on one test subject, and more extensive testing on more subjects is needed. Preferably this should also be tested on Duchenne patients.

A logical next step to continue this research would be to improve the signal from version 3.1. Right now, there is some overlap between the triceps and biceps signals for certain electrodes, and it is unknown why this is the case. This could possibly be improved by moving the ground away from the upper arm, making the electrodes smaller, or making the band asymmetrical, meaning the biceps and triceps electrodes are no longer on the exact opposite sides of the arm. The problems of the ground detaching and the box not fully closing also need to be addressed in the next prototype. Finally for the sake of cost and printing failures, it might be beneficial to experiment with different materials for the electronics box.

Bibliography

[1] MDA, "Duchenne Muscular Dystrophy (DMD)." https://www.mda.org/disease/duchenne-muscular-dystrophy. Retrieved on 10/1/2022.

[2] L. U. M. Centrum, "Duchenne en Becker spierdystrofie." https://www.lumc.nl/patientenzorg/ziektebeelden/duchenne-en-becker-spierdystrofie/. Retrieved on 11/10/2022.

[3] Spierziekten.nl, "DUCHENNE SPIERDYSTROFIE (DMD)." https://www.spierziekten.nl/overzicht/duchenne/. Retrieved on 11/1/2022.

[4] Y. Bionics, "Exoskelet (NL)." https://yumenbionics.com/exoskeleton/. Retrieved on 11/1/2022.

[5] N. Hogan and R. W. Mann, "Myoelectric signal processing: Optimal estimation applied to electromyography - part ii: Experimental demonstration of optimal myoprocessor performance," *IEEE Transactions on Biomedical Engineering*, vol. BME-27, no. 7, p. 396–410, 1980.

[6] G. Wolterink, P. Dias, R. G. Sanders, F. Muijzer, B.-J. v. Beijnum, P. Veltink, and G. Krijnen, "Development of soft semg sensing structures using 3d-printing technologies," *Sensors*, vol. 20, no. 15, p. 4292, 2020.

[7] G. Wolterink, R. Sanders, F. Muijzer, B.-J. van Beijnum, and G. Krijnen, "3d-printing soft semg sensing structures," *2017 IEEE SENSORS*, 2017.

[8] G. Wolterink, P. Dias, R. G. Sanders, F. Muijzer, B.-J. v. Beijnum, P. Veltink, and G. Krijnen, "Development of soft semg sensing structures using 3d-printing technologies," *Sensors*, vol. 20, no. 15, p. 4292, 2020.

[9] J. Lobo-Prat, P. N. Kooren, M. M. H. P. Janssen, A. Q. L. Keemink, P. H. Veltink, A. H. A. Stienen, and B. F. J. M. Koopman, "Implementation of emg- and force-based control interfaces in active elbow supports for men with duchenne muscular dystrophy: A feasibility study," *IEEE Transactions on Neural Systems and Rehabilitation Engineering*, vol. 24, no. 11, p. 1179–1190, 2016.

[10] J. Lobo-Prat, K. Nizamis, M. M. Janssen, A. Q. Keemink, P. H. Veltink, B. F. Koopman, and A. H. Stienen, "Comparison between semg and force as control interfaces to support planar arm movements in adults with duchenne: a feasibility study," *Journal of NeuroEngineering and Rehabilitation*, vol. 14, no. 1, 2017.

[11] C. Meagher, E. Franco, R. Turk, S. Wilson, N. Steadman, L. Mcnicholas, R. Vaidyanathan, J. Burridge, and M. Stokes, "New advances in mechanomyography sensor technology and signal processing: Validity and intrarater reliability of recordings from muscle," *Journal of Rehabilitation and Assistive Technologies Engineering*, vol. 7, p. 205566832091611, 2020.

[12] M. A. Islam, K. Sundaraj, R. Ahmad, N. U. Ahamed, and M. A. Ali, "Mechanomyography sensor development, related signal processing, and applications: A systematic review," *IEEE Sensors Journal*, vol. 13, no. 7, p. 2499–2516, 2013.

[13] R. B. Woodward, M. J. Stokes, S. J. Shefelbine, and R. Vaidyanathan, "Segmenting mechanomyography measures of muscle activity phases using inertial data," *Scientific Reports*, vol. 9, no. 1, 2019.

[14] L. Pan, D. Zhang, N. Jiang, X. Sheng, and X. Zhu, “Improving robustness against electrode shift of high density emg for myoelectric control through common spatial patterns,” *Journal of NeuroEngineering and Rehabilitation*, vol. 12, no. 1, 2015.

[15] M. Rojas-Martínez, L. Y. Serna, M. Jordanic, H. R. Marateb, R. Merletti, and M. Mañanas, “High-density surface electromyography signals during isometric contractions of elbow muscles of healthy humans,” *Scientific Data*, vol. 7, no. 1, 2020.

[16] K. Nizamis, N. H. Rijken, R. van Middelaar, J. Neto, B. F. Koopman, and M. Sartori, “Characterization of forearm muscle activation in duchenne muscular dystrophy via high-density electromyography: A case study on the implications for myoelectric control,” *Frontiers in Neurology*, vol. 11, 2020.

[17] J. Lobo-Prat, M. M. Janssen, B. F. Koopman, A. H. Stienen, and I. J. D. Groot, “Surface emg signals in very late-stage of duchenne muscular dystrophy: a case study,” *Journal of NeuroEngineering and Rehabilitation*, vol. 14, no. 1, 2017.

[18] A. Kapeller, M. H. Nagenborg, and K. Nizamis, “Wearable robotic exoskeletons: A socio-philosophical perspective on duchenne muscular dystrophy research,” *Paladyn, Journal of Behavioral Robotics*, vol. 11, no. 1, p. 404–413, 2020.

[19] B10numbers, “Reaction time.” https://bionumbers.hms.harvard.edu/bionumber.aspx?s=nv=2id=110799. Retrieved on 8/11/2022.

[20] K. Nizamis, “Hand neuro-motor characterization and motor intention decoding in duchenne muscular dystrophy,” 2019.

[21] Santamedical.com, “MEDVICE Manual Blood Pressure Cuff - Universal Size Aneroid Sphygmomanometer - Nurses BP Monitor - Best Adult BP Machine.” https://santamedical.com/products/medvice-manual-blood-pressure-cuff-universal-size-aneroid/-sphygmomanometer-nurses-bp-monitor-best-adult-bp-machine. Retrieved on 14/9/2022.

[22] D. Engineering, “Setting Tool Offsets.” https://support.diabasemachines.com/hc/en-us/articles/360006374514-3-2-Setting-Tool-Offsets. Retrieved on 14/10/2022.

[23] A. Merlo, M. C. Bò, and I. Campanini, “Electrode size and placement for surface emg bipolar detection from the brachioradialis muscle: A scoping review,” *Sensors*, vol. 21, no. 21, p. 7322, 2021.

[24] Bol.com, “Intex Zwembandjes - Large - Oranje - Deluxe - Zwemvleugels - 6-12 jaar - Veiligheid - Zwemmen.” https://www.bol.com/nl/nl/p/intex-zwembandjes-large-oranje-deluxe-zwemvleugels-6-12-jaar- veiligheid- zwemmen/9300000017515193/. Retrieved on 17/10/2022.

[25] G. Wolterink, R. Sanders, F. Muijzer, B.-J. V. Beijnum, and G. Krijnen, “3d-printing soft semg sensing structures,” *2017 Ieee Sensors*, 2017.

[26] G. Wolterink, P. Dias, R. G. P. Sanders, F. Muijzer, B.-J. V. Beijnum, P. Veltink, and G. Krijnen, “Development of soft semg sensing structures using 3d-printing technologies,” *Sensors*, vol. 20, no. 15, p. 4292, 2020.

Conference Paper

Evaluating 3D printed sEMG electrodes with silver ink traces using in-situ impedance measurements

Martijn Schouten*, Philip van de Maat*, Kostas Nizamis† and Gijs Krijnen*
*Robotics And Mechatronics group, University of Twente, Enschede, The Netherlands
†Systems Engineering and Multidisciplinary Design group, University of Twente, Enschede, The Netherlands
Email: m.schouten@utwente.nl

***Abstract* - Surface electromyography (sEMG) is used to determine muscle activity by picking up the associated bio-potentials using skin-mounted electrodes. In this paper, we study how the electrode and skin impedance of 3D printed sEMG electrodes can be improved by comparing traces made of either silver ink or carbon black loaded thermoplastic polyurethane (TPU). To this end we developed a method, using the AC-lead off of the Texas Instruments ADS1298 analog front-end, to continuously determine the complex impedance during sEMG measurements. We observe that the application of silver-ink reduces both the electrode impedance and its variation during isometric contractions.**

Keywords - sEMG, silver ink, 3D printing, BLE, LDM, FFF

I. Introduction

Surface electromyography (sEMG) can be used to measure the activity of muscles, which is useful in for example exoskeleton control [1], [2]. 3D printed sEMG electrodes can be integrated into 3D printed objects [3], [4]. This allows the fabrication of parts with integrated sensors, that are optimized and customized for specific users.

Fused Filament Fabrication (FFF) is a low-cost and accessible fabrication technique, that can be used to print very flexible materials [5]. However, currently, no stretchable high conductivity materials are commercially available. This limits the density of traces that can be printed. On the other hand, stretchable silver inks can be stretched several percent without breaking and are highly conductive [6]. These inks can be printed using liquid deposition modeling (LDM) and therefore are a good candidate for stretchable traces.

One important parameter of a 3D printed sEMG electrode is its impedance [3], [7]. An increased electrode or skin impedance reduces the effective common-mode rejection of the amplifier [8]. It is therefore beneficial to be able to measure the electrode impedance during sEMG measurements. By using frequency-division multiplexing, it is possible to measure impedance and sEMG simultaneously [9].

In this work, a method for simultaneously measuring the electrode and skin impedance during sEMG measurements is proposed and demonstrated. This method uses the AC-leadoff of a commercial ECG front-end. Two sets of electrodes are 3D printed using a multi-material 3D printer equipped with a progressive cavity extruder; one with a conventional carbon black filled thermoplastic polyurethane (TPU) trace and one with a stretchable silver ink trace. The impedance of both is compared using the proposed impedance measurement method.

This work was developed within the Wearable Robotics program, funded by the Dutch Research Council (NWO) and co-funded by TMSi. The authors thank all TMSi employees for their help in the development of the Octopus, as well as Jurgen Bril and Yiming Chen for their contribution to the code.

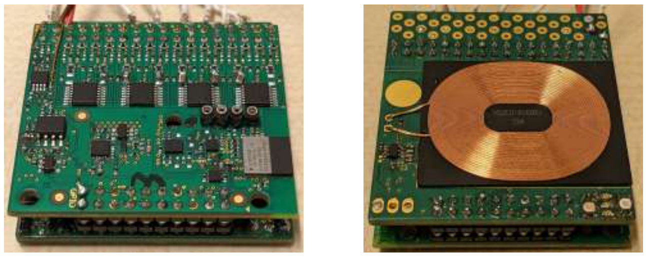

(a) Front side (b) Back side

Fig. 1: The Octopus amplifier used for the simultaneous impedance and sEMG measurements

II. Measurements

A. Impedance measurement

The measurement electronics consist of a custom-developed amplifier called Octopus (Fig. 1). It uses the Texas Instruments ADS1298 Analog Front-End chip, connected to an NRF52832 Bluetooth low energy (BLE) module. The BLE module provides the communication with a PC running windows 10 and a Python program that uses the Bleak library [10] to communicate with the BLE module.

The amplifier is connected to the electrodes using low-noise cables (TMSi). To increase the input impedance of the amplifier, the shield of each coax cable is guarded. To further reduce the capacitance of the ADS1298 chip a negative capacitor circuit [11] has been implemented. The amplifier is converted from a bi-polar into a uni-polar amplifier by determining the average voltage using the Driven Right Leg (RLD) circuitry in the ADS1298 (Fig. 2). This average is subsequently buffered, low pass filtered and connected to the negative inputs of the bipolar channels.

The amplifier makes use of the AC-leadoff feature of the ADS1298. The AC-leadoff function injects a square wave current into the electrodes at a frequency equal to $25\,\%$ of the

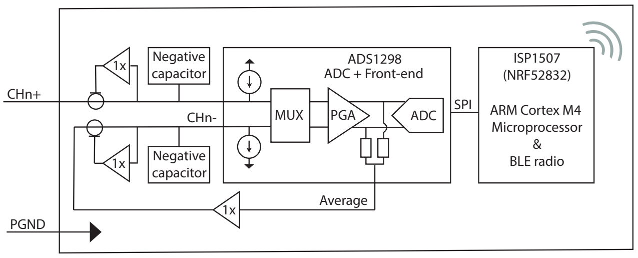

Fig. 2: A block diagram of the Octopus amplifier

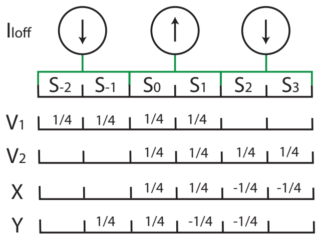

Fig. 3: Illustration showing the method used to filter out the AC-leadoff and determine the impedance.

sampling frequency. By taking the average of four samples (V_n) this square wave can be filtered out again to obtain the sEMG signal. By calculating (V_n) every second sample of S_n, a moving average filter is applied before down-sampling, improving the anti-aliasing performance.

$$
\begin{aligned}
V_1 &= \frac{S_{-2} + S_{-1} + S_0 + S_1}{4} \\
V_2 &= \frac{S_0 + S_1 + S_2 + S_1}{4}
\end{aligned}
\tag{1}
$$

To calculate the impedance a digital square wave lock-in algorithm [12], [13] is implemented, using that the current sources change direction synchronously with the sampling frequency (Fig. 3). The resistance (X) and reactance (Y) are calculated respectively as the in- and out-of-phase components using:

$$
\begin{aligned}
X &= \frac{S_0 + S_1 - S_2 - S_3}{4I_{\text{loff}}} \\
Y &= \frac{S_{-1} + S_0 - S_1 - S_2}{4I_{\text{loff}}}
\end{aligned}
\tag{2}
$$

with I_{loff} the lead-off current. The measurements in this work used a I_{loff} of $24\,\text{nA}$ and integrate the impedance over 10 mains cycles, or $200\,\text{ms}$. Because of the EMI-reduction filter in the ADS1298 and the $3.2\,\text{k}\Omega$ resistor which is placed in series with each input for safety, it is expected that the measured resistance will be offset by $16.4\,\text{k}\Omega$.

B. Calibration

The impedance measurement is calibrated using 4 resistor-capacitor networks. The exact component values in the networks were measured using a HAMEG HM8118 Programmable LCR bridge [14]. The resulting values can be found in Table I. Table II shows which of the networks were connected between channel 3 (CH3) and patient ground (PGND), as well as between channel 4 (CH4) and PGND.

TABLE I: The values of the component networks

	Z1	Z2	Z3	Z4
R (kΩ)	26.61	26.74	9.90	9.85
C (nF)	15.79	14.53	47.47	46.43

TABLE II: The impedance connected between CH3, CH4 and PGND.

CH3 to PGND	0	Z1	0	Z1	Z3	0	Z3
CH4 to PGND	0	0	Z2	Z2	0	Z4	Z4

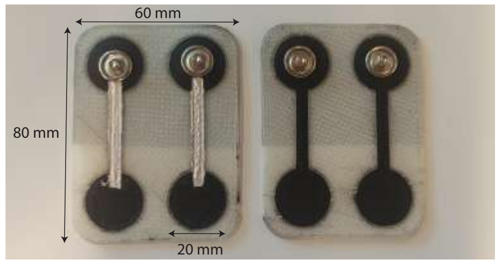

Fig. 4: The electrode pairs using a trace made of silver ink (left) and PI-ETPU (right).

C. Fabrication

To print the electrode sets an H-series 3D printer (Diabase Engineering) equipped with a Viscotec Viprohead 3 is used. To mount the Viprohead on the 3D printer a custom bracket [15] was 3D printed and the software running on the printer was modified [16]. The extruder was equipped with a Viscotec Preeflow super high precision dispense nozzle with a $609\,\mu\text{m}$ hole to be able to extrude the highly viscous ($10\,\text{Pa s}$ [17]) silver ink.

To determine whether silver ink can be used as a trace material two electrode sets have been printed. One uses CI-1036 stretchable silver-ink (Engineered Conductive Materials) as a trace material and one uses PI-ETPU 85-700+ (Palmiga Innovations). The actual electrodes consisted of PI-ETPU, printed with 100 percent infill and a thickness of $750\,\mu\text{m}$. The electrodes were mechanically connected by transparent X60 Ultra-Flexible Filament (Diabase Engineering). To create a reliable and sturdy connection with the stretchable 3D printed sample a snap button (KOH-I-NOOR, $11\,\text{mm}$) was pushed through the 3D printed band onto a layer of PI-ETPU. The assembled bands were then annealed at $100\,^{\circ}\text{C}$ for $30\,\text{min}$ in a Memmert UF30 oven. After annealing, a piece of duct tape was added to insulate the snap buttons from the skin. A picture of the prints can be seen in Fig. 4.

D. Measurement setup

During the measurements, the electrodes were placed on the skin above the muscle belly of the Biceps Brachii underneath a sweatband (Fig. 5). The skin above the Biceps muscle was cleaned with alcohol prior to the electrode placement. The snap buttons were kept outside the sweatband and were connected to two uni-polar channels of the Octopus. The ground of the Octopus is connected to the wrist of the same arm using a TMSi ground bracelet. All measurements were performed on a single subject (Male, 24 years). To check the stability of the electrode impedance 5 isometric contractions

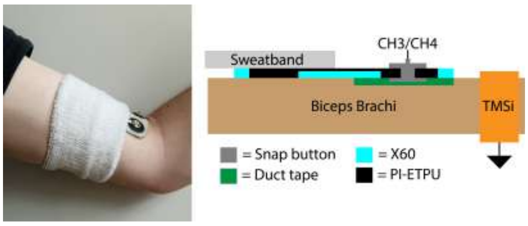

Fig. 5: A picture and schematic cross-section of an electrode pair placed on the biceps underneath the sweatband

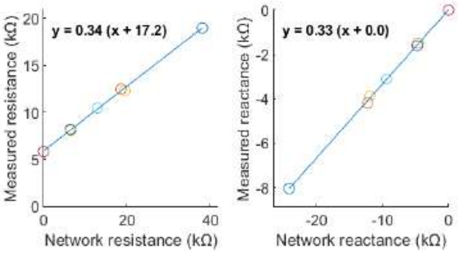

Fig. 6: The measured vs the expected impedance of the resistance networks. A linear fit through the points is used to calibrate the impedance measurement.

of approximately 1 s at 100 % maximum voluntary contraction were performed. To be able to access the repeatability of the results, the experiment was repeated 5 times and in between the electrodes were removed and placed back.

To calculate the sEMG envelope, motion artifacts and baseline offset were first removed from the data by high pass filtering with a 20 Hz 200th order zero-phase FIR filter. A frequency of 20 Hz was used to be sure that the 0.5 Hz motion and its higher harmonics were filtered out. The envelope of the signal is determined by low pass filtering the absolute value of the signal with a 5 Hz second-order Butterworth filter.

III. Results and discussion

A. Calibration

The measured impedance is plotted against the impedance measured by the LCR bridge in Fig. 6. A linear fit is performed and used to calibrate the impedance measured. The series resistance was found to be 17.2 kΩ. The 0.8 kΩ difference with the expected series resistance might be due to the on-resistance of the multiplexer in the ADS1298. The calibration showed that the measured voltage was 33-34 % of the expected voltage. This is expected to be because of the attenuation of the sinc-filter in the ADS1298 and because the ADC measures the mean of the rectified first harmonic.

B. Impedance measurement

Fig. 7 shows the absolute value and phase of the measured impedance as well as the simultaneously measured sEMG during 5 isometric contractions, for both the electrode set with a silver ink trace and a PI-ETPU trace. The mean absolute impedance and phase are plotted in Fig. 8. The mean absolute impedance over all measurements was 72 kΩ with silver ink and 443 kΩ with PI-ETPU. In this figure, the error bars indicate the minimum and maximum impedance measured during

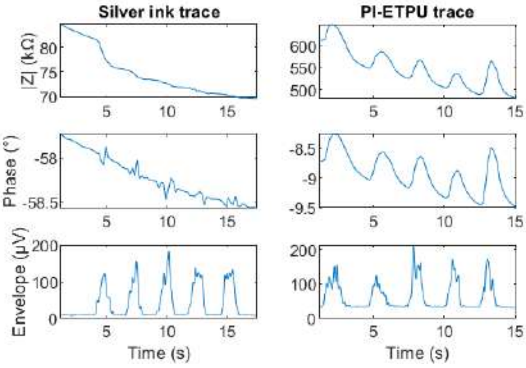

Fig. 7: Mean absolute value and phase of the electrode and skin impedance measured simultaneously with the envelope of the EMG signal.

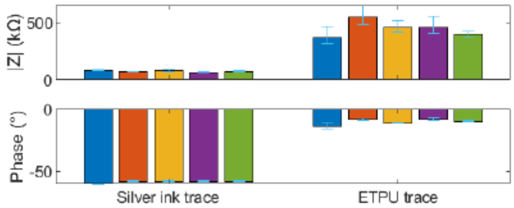

Fig. 8: Absolute value and phase of the combined electrode skin impedance as calculated by taking the mean over time of the mean impedance of the left and right electrode. Error bars indicate the minimum and maximum values.

each measurement. It was noted that during each measurement the electrode impedance drifted downwards. With silver ink the average change in absolute impedance was 7 kΩ (10 %) versus 121 kΩ (27 %) with PI-ETPU.

It should also be noted that the electrode impedance was measured only at 250 Hz and although this is within the sEMG bandwidth, the impedance may vary within this bandwidth. Furthermore, although the results were repeatable after replacing the electrodes multiple times, the experiment has only been performed on a single subject. Therefore, any effects due to variation between subjects are still to be investigated.

IV. Conclusions

In this paper, it was shown that impedance can be measured by applying a digital lock-in algorithm to the AC-leadoff detection of a commercial ECG frontend. It was also shown that this technique can be used to measure the combined skin and electrode impedance at the same time as the sEMG signal.

Next, a multi-material 3D printer combining both FFF and LDM was used to print an electrode set with both silver ink and PI-ETPU wires. It was shown, for the first time, during sEMG measurements, that the silver ink wires significantly reduce both the electrode impedance and its variations.

Furthermore, it was demonstrated that a stable impedance measurement can be obtained during isometric contraction using 3D printed electrodes with silver ink traces, applied under a sweatband. This opens the way to 3D printed bands with multiple sEMG sensors with more complex wiring and better signals, due to lower electrode and skin impedance.

REFERENCES

[1] K. Nizamis, J. Lobo-Prat, A. Q. Keemink, R. Carloni, A. H. Stienen, and B. F. Koopman, "Switching proportional emg control of a 3d endpoint arm support for people with duchenne muscular dystrophy," in *2015 IEEE International Conference on Rehabilitation Robotics (ICORR)*, pp. 235–240, 2015. DOI: 10.1109/ICORR.2015.7281205.

[2] T. Lenzi, S. M. M. De Rossi, N. Vitiello, and M. C. Carrozza, "Intention-based emg control for powered exoskeletons," *IEEE Transactions on Biomedical Engineering*, vol. 59, no. 8, pp. 2180–2190, 2012. DOI: 10.1109/TBME.2012.2198821.

[3] G. Wolterink, P. Dias, R. G. P. Sanders, F. Muijzer, B.-J. v. Beijnum, P. Veltink, and G. Krijnen, "Development of soft semg sensing structures using 3d-printing technologies," *Sensors*, vol. 20, p. 4292, July 2020. DOI: 10.3390/s20154292.

[4] R. Zhang, V. Kolbin, M. Süttenbach, M. Hedges, and O. Amft, "Evaluation of 3d-printed conductive lines and emg electrodes on smart eyeglasses frames," in *Proceedings of the 2018 ACM International Symposium on Wearable Computers*, (New York, NY, USA), p. 234–235, Association for Computing Machinery, 2018. DOI: 10.1145/3267242.3267289.

[5] M. Schouten, G. Wolterink, A. Dijkshoorn, D. Kosmas, S. Stramigioli, and G. Krijnen, "A review of extrusion-based 3d printing for the fabrication of electro- and biomechanical sensors," *IEEE Sensors Journal*, vol. 21, no. 11, pp. 12900–12912, 2021. DOI: 10.1109/JSEN.2020.3042436.

[6] M. Borghetti, T. Fapanni, N. F. Lopomo, E. Sardini, and M. Serpelloni, "A preliminary study on aerosol jet-printed stretchable dry electrode for electromyography," in *Applications in Electronics Pervading Industry, Environment and Society*, pp. 292–296, Springer International Publishing, 2021. DOI: 10.1007/978-3-030-66729-0_36.

[7] M. Yamagami, K. M. Peters, I. Milovanovic, I. Kuang, Z. Yang, N. Lu, and K. M. Steele, "Assessment of dry epidermal electrodes for long-term electromyography measurements," *Sensors*, vol. 18, no. 4, 2018. DOI: 10.3390/s18041269.

[8] A. C. Metting Van Rijn, A. Peper, and C. A. Grimbergen, "High-quality recording of bioelectric events - Part 1 Interference reduction, theory and practice," *Medical & Biological Engineering & Computing*, vol. 28, no. December, pp. 389–397, 1990. DOI: 10.1007/BF02441961.

[9] Y. Jiang, M. Togane, B. Lu, and H. Yokoi, "semg sensor using polypyrrole-coated nonwoven fabric sheet for practical control of prosthetic hand," *Frontiers in Neuroscience*, vol. 11, 2017. DOI: 10.3389/fnins.2017.00033.

[10] D. Lechner, H. Blidh, and K. Davis, "Bleak." [Online]. Available: https://github.com/hbldh/bleak [Accessed: 17-Aug-2022].

[11] T. Kimura, H. Watanabe, M. Adachi, S. Kuriki, and A. Ueno, "Performance evaluation of electroencephalograph with negative capacitance converter," *5th 2012 Biomedical Engineering International Conference, BMEiCON 2012*, 2012. DOI: 10.1109/BMEiCon.2012.6465475.

[12] D. Afanassyev and V. Rabyk, "A digital lock-in technique for small signal detection with square wave reference over a wide frequency range," in *2018 14th International Conference on Advanced Trends in Radioelecrtronics, Telecommunications and Computer Engineering (TCSET)*, pp. 480–483, 2018. DOI: 10.1109/TCSET.2018.8336245.

[13] D. Dobrev, T. Neycheva, and N. Mudrov, "Digital lock-in techniques for adaptive power-line interference extraction," *Physiological Measurement*, vol. 29, pp. 803–816, June 2008. DOI: 10.1088/0967-3334/29/7/009.

[14] HAMEG Instruments GmbH, "R&S HM8118 Programmable LCR-Bridge User Manual." [Online]. Available: https://scdn.rohde-schwarz.com/ur/pws/dl_downloads/dl_common_library/dl_manuals/gb_1/h/hm8118_1/HM8118_UserManual_de_en_06.pdf [Accessed: 17-Aug-2022].

[15] M. Schouten and D. Kosmas, "Viscotec viprohead 3 mount for diabase h-series 4." [Online]. Available: https://grabcad.com/library/viscotec-viprohead-3-mount-for-diabase-h-series-4-1 [Accessed: 26-Aug-2022].

[16] M. Schouten and D. Kosmas, "H-series-configuration." [Online]. Available: https://github.com/martijnschouten/H-Series-Configuration/tree/H4052-NIFTy-paste [Accessed: 26-Aug-2022].

[17] Engineered Conductive Materials, LLC, "Technical Data Sheet CI-1036 Highly Conductive, Highly Flexible Silver Ink," 2010.